CORNELL AERONAUTICAL LABORATORY, INC.

Report No. AF-1285-A-4

HYPERSONIC FLOW WITH COMBINED LEADING-EDGE BLUNTNESS AND BOUNDARY-LAYER DISPLACEMENT EFFECT

H.K. Cheng

August 1960

Contract Nonr-2653(00)
Task NR 061-106

CORNELL AERONAUTICAL LABORATORY, INC.
BUFFALO, NEW YORK

REPORT NO. AF-1285-A-4

HYPERSONIC FLOW WITH COMBINED LEADING-EDGE BLUNTNESS AND BOUNDARY-LAYER DISPLACEMENT EFFECT

AUGUST 1960

BY: Hsien K. Cheng
Hsien K. Cheng

APPROVED BY:
A. Hertzberg, Head
Aerodynamic Research Dept.

This report is based on research sponsored by the U.S. Navy through the Office of Naval Research, Contract Nonr-2653(00)

FOREWORD

The study on which this report is based constitutes a part of the research program sponsored by the U. S. Navy through the Office of Naval Research (Fluid Dynamics Branch) under Contract No. Nonr-2653(00).

The author would like to take this opportunity to acknowledge the assistance of Mrs. Angela Chang who undertook most of the detailed analysis, and Mr. F. Butler for programming the digital machine computations. He also found during the course of investigation his discussions with Drs. W. E. Gibson, J. G. Hall and F. K. Moore most helpful.

ABSTRACT

A theoretical study is made of hypersonic flows over thin bodies subject to the combined effect of leading-edge bluntness, boundary-layer displacement as well as surface incidence. Within the scope of the boundary-layer theory and the hypersonic small-disturbance theory, an approach is developed based on a flow model consisting of three adjoining regions: an inner laminar boundary layer; an outer (detached) shock layer; and between these two, a low-density entropy layer. This approach allows simultaneous treatment of the boundary layer and its outer inviscid flow field in a manner consistent with the Newtonian shock-layer approximation.

The theory pertaining to the leading approximation for strong shock and $\gamma \to 1$ is completely developed and its simplicity permits solutions to a number of problems of interest. For the flat plate at zero incidence, the theory yields a solution agreeing with the blast-wave theory at one limit and the strong inviscid-viscous interaction theory at the other. Results are also obtained for the flat plate at incidence. The results for the pure inviscid flows with tip-bluntness effect exhibit an oscillatory decay in pressure on slender cone and wedge afterbodies. This phenomenon signifies an idealized form of re-impingement of the shock layer on the afterbody at glancing incidence.

Complementary to the aforementioned study, an examination is made of the similitude of hypersonic boundary layers, taking specifically the leading-edge bluntness into account. Rules for correlating pressure, shock shape, skin friction and heat-transfer rate are given. The simplification of these rules for flows with strong shock waves is pointed out.

TABLE OF CONTENTS

TABLE OF CONTENTS (Contd)

NOTATION

a_∞	speed of sound in the free stream
A, B	constants
c_f	$\left(\mu \frac{\partial u}{\partial y}\right)_w \Big/ \frac{1}{2}\rho_\infty U^2$, the skin-friction coefficient
c_H	$\left(k \frac{\partial T}{\partial y}\right)_w \Big/ \rho_\infty U(H_\infty - H_w) = q/\rho_\infty U(H_\infty - H_w)$, the surface heat-transfer coefficient
c_p, c_v	specific heats of the gas at constant pressure and at constant volume, respectively
C	constant of proportionality in the linear viscosity temperature relation $\mu/\mu_\infty = CT/T_\infty$
C_*	$\frac{\mu(T_*)}{\mu(T_\infty)} \cdot \frac{T_\infty}{T_*}$
D_N	drag of the blunt leading edge or nose
e	specific internal energy of the gas
f, F	symbols representing certain functions of the variables involved in Eqs. (4.15), (5.1) and (5.2)
h	specific enthalpy
H	$h + \frac{1}{2}(u^2 + v^2)$, total specific enthalpy
J_σ, Y_σ	σ^{th} order Bessel's functions of the first and second kind, respectively
k	$D_N \Big/ \frac{1}{2}\rho_\infty U^2 t (\pi t/4)^{\nu}$, leading-edge (nose) drag coefficient
K_ϵ	$M^{\frac{3+\nu}{1+\nu}} (\epsilon k)^{\frac{1}{1+\nu}} \frac{t}{\nu}$, a parameter controlling inviscid tip-bluntness effect
L	reference length
m	constant associated with the streamline in the entropy layer
M	U/a_∞, free-stream Mach number

p	pressure
P_r	Prandtl number $\mu c_p/\kappa$
R	gas constant in the equation of state
Re	Reynolds number
t	thickness of the blunt leading edge or nose
T	temperature
T_*	$T_0\left[1+3\frac{T_w}{T_0}\right]\Big/6$, a reference temperature for defining C
u, v	velocity components parallel to the x and y axes, respectively
U	the value of u in the free stream
Δu	$u - U$, the streamwise perturbation velocity
x, y	rectangular coordinates in directions parallel and normal, respectively, to the free-stream velocity with the origin at the nose
Y_b, Y_e, Y_s, Y_w	the y ordinates of the inner edge of the entropy layer, the outer edge of the entropy layer, the shock, and the body surface, respectively
z, ζ	the variables related to Y_e and x , respectively, as defined in the text
α	the angle of attack of the flat plate. Positive α refers to compression or wedge flow over the surface in question; also half-cone angle
γ	c_p/c_v , specific-heat ratio
δ, δ_*	the boundary-layer thickness and displacement thickness, respectively
$\epsilon, \epsilon_\infty$	$\frac{\gamma-1}{\gamma+1}$, $\frac{\gamma_\infty-1}{\gamma_\infty+1}$, respectively
θ	the shock angle, i.e. dY_s/dx , which may be taken as the typical flow-deflection angle

Θ	$\frac{H - H_w}{H_\infty - H_w}$
Φ	a function whose derivative $\partial\Phi/\partial\bar{\eta}$ is $\frac{u}{U}$
κ	thermal conductivity of the gas
μ	viscosity of the gas
λ, ϕ	certain variables in Section 4
ξ, η	two spatial variables used in the boundary-layer analysis, see Eq. (2.1)
ν	a number which is zero for plane flows and unity for axisymmetric flows
ρ	gas density
Π	$K_\epsilon / \bar{\gamma}_\epsilon^2$
τ	a body thickness parameter used in the similitude consideration (for the wedge and cone, $\tau = \alpha$)
$\bar{\gamma}, \bar{\gamma}_L, \bar{\gamma}_t$	$M^3\sqrt{\frac{C}{Re_x}}$, $M^3\sqrt{\frac{C}{Re_L}}$, $M^3\sqrt{\frac{C}{Re_t}}$, respectively
γ_ϵ	$\epsilon\,(0.664 + 1.73\,\frac{T_w}{T_o})\,\bar{\gamma}$, a parameter governing the boundary-layer displacement effect
ω	the constant exponent in the relation $\mu \propto T^\omega$

Subscript:

b	pertaining to the inner edge of the entropy layer
B	pertaining to the Blasius solution
e	at the outer edge of the entropy layer
L	based on the reference length ($x = L$)
N	pertaining to the condition behind the strongest part of the shock at the nose

s	behind the shock (at x)
t	based on the nose thickness ($x = t$)
w	at the body surface or wall
δ	at the outer edge of the boundary layer
o	pertaining to the free-stream stagnation conditions (for the temperature)
∞	pertaining to the free-stream condition
$*$	based on the reference temperature T_*

LIST OF ILLUSTRATIONS

SECTION 1

INTRODUCTION

Two outstanding features characterize the hypersonic flow around a thin body. One is the displacement effect of the boundary layer and the other is the downstream influence of a small, but blunt, nose or leading edge. The pronounced displacement effect is related to the viscous dissipation of the high-speed flow, which raises the local temperature and thus the kinematic viscosity. The lateral extent of the hypersonic boundary layer may therefore become comparable, or greater than, the thickness of the thin body, and an interaction of the inviscid and viscous flow regions must take place. The importance of the leading-edge bluntness may be perceived from the connection between the energy gained by the cross-flow field and the nose drag. Since the drag of a blunt nose is rather high, the work done by it alone may account for a sizable portion of the total energy delivered to the fluid. The unsteady motion observed in the cross-flow plane, that is, a plane fixed with respect to the ambient fluid and transverse to the direction of motion, may therefore be compared with that of a blast wave generated by instantaneous release of energy of an amount proportional to the nose drag. For hypersonic flight of slender bodies, leading-edge bluntness is generally essential for heat-transfer control, while for flight at relatively high altitude, the boundary-layer displacement effect is important. This study will consider hypersonic flows in which both of these phenomena are present.

There is a body of theory dealing with each of these two effects as independent phenomena. For the boundary-layer displacement problem taken separately, we have the rather extensive works on strong and weak interactions of the invis-

cid and boundary-layer flows over a (sharp-edged) flat plate, as well as treatments of related problems[1-17]. These theories provide an account of the self-induced pressure in the outer flow associated with the displacement effect of the boundary layer. From the literature on the subject, the early contributions of Shen[1,4], Lees and Probstein[3,6], Li and Nagamatsu[5], and also the definitive work of Stewartson[9] should be noted. Taking the bluntness effect separately, we have the strong blast-wave theories of Lin[18], Lees and Kubota[19] and others[20-24]. These works make use of the analogy between the transient cross-flow field downstream of a blunt nose and the flow field produced by a violent explosion of the type previously treated by Taylor[25,26].

On the other hand, for the problems in which both the displacement and bluntness effects are important, there has not been any satisfactory theory. A theory accounting simultaneously for both effects is essential not only for its practical implication, but also because the task of isolating these two effects in hypersonic flow is generally not simple, even under laboratory conditions[27-31]. The aim of this paper is to present a simplified but consistent approach to the problem which will render possible the study of interaction of the boundary layer with the outer flow under the influence of leading-edge bluntness as well as afterbody geometry.

A continuum flow model consisting of a laminar boundary layer adjacent to the slender body and an inviscid outer flow field will be assumed for this theoretical study. Since the Mach numbers considered are high, and the bodies thin, the lateral extent of the flow field bounded by the bow shock is small. Our analysis may therefore be carried out within the scope of the boundary-layer theory[4,6] and the (inviscid) hypersonic small-disturbance theory[32-34]. Within

this framework, two complementary studies are made. First, and the major part of our analysis, is the development of an approach which takes account of the combined effect of boundary-layer displacement, leading-edge bluntness, and body thickness. To achieve this end, certain approximations and simplifications will be introduced. The second study is concerned with hypersonic similitude when both boundary-layer and tip-bluntness effects are present, and with simplification of the similarity law for flows with strong shock waves. For this similitude consideration, a number of the assumptions introduced in the first study are not required.

Underlying the present approach are the two basic concepts: a local similarity in the boundary layer and a detached shock layer in the outer inviscid flow. Both of these concepts are desirable for a development consistent with the so-called Newtonian shock-layer approximation[35-40]. The consistency between local similarity and the shock-layer approximation has, in fact, been discussed earlier[41]. The concept of a detached shock layer, which includes the so-called "free layers"[39,41] as special cases, is a necessary modification of the shock-layer theory to allow treatment of tip bluntness.

A similar treatment of the tip-bluntness effect has been given previously by Chernyi[21,22]. The essential idea of a detached shock layer is implicit in his integral method for hypersonic inviscid flows. While Chernyi's method and the present analysis are equivalent in the idealized limit $\gamma \longrightarrow 1$, they differ in the higher order approximation for γ not close to unity. It may also be pointed out that the inviscid tip-bluntness effect has been studied recently by Guiraud[42,43]. Here, the idea of a detached shock layer was employed, and certain equations obtained are very similar to those to be developed later in this re-

port. Guiraud's study does not lead to an explicit solution of the problem, however.

Throughout the present analysis an ideal gas with constant specific heats will be assumed ahead of and behind the shock (although γ may change across the shock). In order to arrive at a simple form of local similarity in the boundary layer, the Prandtl number is taken to be unity, the body temperature is assumed to be uniform, and a linear viscosity-temperature relation is adopted. The present study is primarily concerned with plane, steady flows. For the purpose of comparing plane and axisymmetric flows for the inviscid tip-bluntness effect, however, the problem of a blunted slender cone is also studied along with the corresponding problem of plane flow over a blunted wedge.*

The three requirements which control the accuracy of the following analysis of the present flow model may be expressed as follows:

(a) The disturbance velocity $\frac{\Delta u}{U} \equiv \left[\frac{u}{U} - 1\right]$, as well as the square of the flow angle, in the inviscid flow field must be negligibly small in comparison to unity.

(b) The bow shock wave must be sufficiently strong.

(c) The specific heat ratio γ must be sufficiently close to unity.

The first requirement implies exclusion of the blunt-nose region itself from the present enquiry, and we will deal only with its downstream effect. The consistency of these requirements and the degree of the approximation involved will be examined later. The zero-order theory, which is to be studied in detail,

---

* The axisymmetric problem involving boundary-layer displacement is complicated by the transverse-curvature effect. In principle, however, a modified form of the local similarity can be obtained for the boundary layer, although it may lose the appeal of simplicity.

pertains to the leading approximation under the last two requirements cited, and may therefore be compared with the classical result of Busemann[35-40] (Newtonian-Plus-Centrifugal-Force).

In view of the continuum assumption, the present theoretical model cannot be used as a valid description of flow phenomena when the molecular nature of the gas is manifested. On the other hand, the effects of velocity-slip, and temperature-jump, as well as of the "vorticity interaction" which precedes the breakdown of the usual continuum model, may be seen to belong to the same, or higher, order as the error in the standard boundary-layer approximation[13,16,44]. We may therefore expect the continuum theory to remain meaningful so long as there exists a sufficiently thin boundary layer, and this condition is implied by requirement (a). Based on the solutions obtained, it is possible to define a domain of validity for the present continuum flow model in terms of the Mach and Reynolds numbers of the free stream. It may be seen that this domain is large enough to permit many useful applications. The adoption of the unit Prandtl number and a linear viscosity-temperature relation may seem at first sight to be oversimplifying the problem. As examples will reveal, these simplifications are not likely to affect the skin friction, heat transfer, and the displacement thickness in a significant way, particularly, when an appropriate reference temperature is chosen for the viscosity-temperature relation. We may notice also that for the present analysis, these two assumptions are not strictly necessary. Analyses similar to the present one may be carried out for an arbitrary but constant Prandtl number and a more general viscosity law with no apparent difficulty. Another limitation of the present study is, of course, the assumption of constant specific heats. The gas behind the normal shock in

front of a blunt nose, under most circumstances, will be in a dissociated, or internally excited state; the specific heat ratio of the gas will be closer to unity than that under standard atmospheric condition. Generally speaking, the shock-layer approximation may improve as a result of the real-gas properties at high temperature. Strictly speaking, however, the specific heat ratio or its equivalent cannot generally be taken as constant for the entire flow field. If the flow field over the slender afterbody can be assumed to be near local thermal equilibrium, and if the body temperature is sufficiently low, the real-gas effects may not be critical since the local temperature downstream is considerably lower than the stagnation temperature at the nose. In any case, the approach presented herein may still be employed to simplify the analysis, although it may not lead directly to a solution. This point will be discussed further.

A somewhat shortened version of this investigation, together with experimental results, has been presented in Ref. 45*. In addition to the inclusion of tip-bluntness effects in axisymmetric flows, further discussion and clarification not given in Ref. 45 will be taken up here.

In the following sections, the local similarity in the boundary layer and its consistency with the inviscid shock-layer approximation will first be discussed. The theory of a detached shock layer will next be considered. The zero-order theory for the complete problem will then be developed and applied to particular cases of interest.

---

* The experimental study described in Ref. 45 was conducted in the Cornell Aeronautical Laboratory 11 x 15-inch Hypersonic Shock Tunnel under the sponsorship of the U. S. Air Force Office of Scientific Research.

SECTION 2

THE LOCAL SIMILARITY AND THE SHOCK-LAYER APPROXIMATION

The idea of assuming a local similarity in the boundary layer as a means of estimating heat-transfer rates on blunt bodies at high speed was first proposed by Lees[46] and utilized by others[47,48]. Lees observed that the enthalpy distribution in the boundary layer is rather insensitive to pressure gradient, particularly if the boundary layer is cooled. For most engineering application, it suffices to ignore the pressure gradient, except for its effects on changing the local Reynolds number. In this case the problem is reducible to that of a flat plate, and for this problem, a self-similar solution exists if the wall-to-stagnation temperature ratio is constant along the plate.*

It is essential to recognize that in the present study, where only thin bodies are considered, the pressure gradient is unimportant not primarily because the wall is made cold, but because the direct effect of pressure gradient on the hypersonic boundary layer is at most of the order

$$\epsilon \equiv \frac{\gamma - 1}{\gamma + 1}$$

The condition of small ϵ is a requirement in existing shock-layer theories for inviscid hypersonic flows[35-40]. It is natural to treat the present boundary-layer problem by an analogous perturbation procedure which uses ϵ as a controlling parameter. The argument used for the local similarity method in blunt body applications is avoided in the present approach.

---

* In a more specific sense, the similarity under discussion should be termed the "local flat-plate similarity".

The foregoing considerations are readily seen after transforming the variables x , y in the boundary layer as follows:

$$\left.\begin{aligned} \xi &= \int_0^x C\,\frac{p}{p_\infty}\,\frac{dx}{L} \\ \eta &= \sqrt{Re_L}\int_0^y \left(\frac{\rho}{\rho_\infty}\right)\frac{dy}{L}\Big/\sqrt{\int_0^x C\,\frac{p}{p_\infty}\,\frac{dx}{L}} \end{aligned}\right\}$$

where

$$Re_L \equiv \frac{\rho_\infty U_\infty L}{\mu_\infty}$$

Assuming a linear viscosity temperature relation

$$\frac{\mu}{\mu_\infty} = C\,\frac{T}{T_\infty}$$

and a unit Prandtl number, the system of differential equations governing the boundary-layer problems in plane flow is reduced to

$$2\Phi_{\eta\eta\eta} + \Phi\Phi_{\eta\eta} - 2\xi\left[\Phi_\eta\Phi_{\xi\eta} - \Phi_\xi\Phi_{\eta\eta}\right] = \epsilon\left[\frac{2\,dp/dx}{p^2}\int_0^x p\,dx\right]\left[\frac{T_w}{T_0} + \left(1-\frac{T_w}{T_0}\right)\Theta - \Phi_\eta^2\right] , \tag{2.1a}$$

$$2\Theta_{\eta\eta} + \Phi\Theta_\eta - 2\xi\left[\Phi_\eta\Theta_\xi - \Phi_\xi\Theta_\eta + \Phi_\eta\Theta\,\frac{d}{d\xi}\ln\left(1-\frac{T_w}{T_0}\right)\right] = 0$$

and the boundary conditions to

$$\left.\begin{aligned} \Phi = \Phi_\eta = \Theta = 0 \qquad &\text{at} \qquad \eta = 0 \\ \Phi_\eta = \Theta = 1 \qquad &\text{at} \qquad \eta = \infty \end{aligned}\right\} \tag{2.1b}$$

where

$$\Phi_\eta = \frac{u}{U} \qquad\qquad \Theta = \frac{H - H_w}{H_\infty - H_w}$$

In arriving at these equations, quantities of orders $1/M^2$ and $\Delta u_\delta/U$ higher than the remaining terms have been neglected. Implicit in Eq. (2.1) is the fact that within the degree of approximation afforded by the boundary-layer analysis, the normal pressure gradient can be ignored. For the neglect of the pressure variation across the boundary layer, an extremely thin boundary layer is not strictly necessary. Rather, the neglection depends on the density level within the hypersonic boundary layer being relatively low. Therefore the pressure may be taken as a function of x alone even when the boundary-layer thickness becomes comparable to the lateral extent of the outer flow[4,6].

Now, consider the situation when ϵ is also small. Except for the parameter ϵ itself, all terms appearing in Eq. (2.1) will remain of order unity. That is, they will be independent of ϵ in the limit $\epsilon \longrightarrow 0$. In this limit, the right-hand member of Eq. (2.1a), which involves the pressure gradient, vanishes with ϵ. The leading approximation to the solution of the system Eq. (2.1) for small ϵ will therefore be independent of ϵ and is, in fact, governed by the Blasius equation

$$\left.\begin{aligned} 2\,\Phi_B''' + \Phi_B\,\Phi_B'' &= 0 \\ \Phi_B(0) = \Phi_B'(0) = \Phi_B'(\infty) - 1 &= 0 \end{aligned}\right\} \qquad (2.2)$$

with $\Theta_B = \Phi_B'$. The problem of determining the higher-order approximation is equivalent to finding a correction to the classical flat-plate solution for a slight nonuniformity of the outer inviscid flow. The nonhomogeneous term appearing on the right of Eq. (2.1) reveals clearly the role of the wall-to-stagnation temperature ratio in controlling the degree of approximation of local boundary-layer similarity. Changing T_w/T_o from unity to zero may typically reduce the correction term by 75%.

Neglect of the pressure-gradient term in the boundary-layer momentum equation has also been employed by Lees[6] to simplify the problem of strong shock boundary-layer interaction. For this problem, however, a self-similar solution exists even with the pressure gradient retained. The theoretical justification for the neglect of pressure gradient to cases involving arbitrary pressure distribution on the basis of the shock-layer theories has only been pointed out quite recently[41].

The mathematical problem of determining the higher-order approximation is one that involves solution to a linear partial differential equation. An alternative which avoids solving the partial differential equation is, of course, the momentum-integral method usually adopted in boundary-layer analyses. For the purpose of determining pressure, skin friction, and surface heat-transfer rate for the present problem, this method may be sufficient, as has been demonstrated by Stewartson's analysis for the strong interaction problem of the flat plate[9]. The scheme arrived at recently by Moore[49], which accounts for the first-order correction to the local similarity, is essentially one of a similar nature. When the momentum-integral method is employed, the local similarity assumption is no longer necessary, even as a leading approximation (for small ϵ).

In the leading approximation for small ϵ , the surface heat-transfer rate, the skin friction, and the displacement thickness of the boundary layer are determined explicitly from the pressure distribution. For the case of plane flow

$$M^3 c_H \approx 0.332\, \bar{\gamma}_L \frac{p/p_\infty}{\sqrt{\int_0^x \frac{p}{p_\infty}\frac{dx}{L}}}$$

$$c_f \approx 2 c_H \qquad (2.3)$$

$$M\frac{\delta_*}{L} \approx \epsilon\left(0.664 + 1.73\,\frac{T_w}{T_0}\right)\bar{\gamma}_L \frac{\sqrt{\int_0^x \frac{p}{p_\infty}\frac{dx}{L}}}{p/p_\infty}$$

where

$$\bar{\chi}_L \equiv M^3 \sqrt{\frac{C}{Re_L}}$$

These results, in view of the approximations involved, will be subject to errors of order ϵ and $\Delta u_\delta / U$. The usual errors inherent in the boundary-layer equations as well as errors from possible slip, temperature-jump, and vorticity effects, will presumably be no larger than those incurred by the approximation $u_\delta \simeq U$.[13,16,44] The magnitude of $\Delta u_\delta / U$ will be examined later.

Before proceeding to the analysis of the inviscid flow region, the choice of a reference temperature for the determination of the constant in the linear viscosity-temperature relation will be discussed. The assumption of such a viscosity law may seem to be unrealistic since the temperature variation within the hypersonic boundary layer is quite large and the detail of viscosity law may be important. The approximation may be considerably improved by choosing the constant C to represent correctly the value of viscosity at an appropriate reference temperature. Instead of choosing the wall temperature as a reference, as was proposed earlier by Chapman and Rubesin[50] and adopted later by others for hypersonic applications, we recommend a reference temperature T_* defined by

$$T_* \equiv T_e \left[1 + 3 \frac{T_w}{T_e} \right] / 6 \qquad (2.4)$$

whence

$$C = C_* \equiv \frac{T_\infty}{T_*} \frac{\mu(T_*)}{\mu(T_\infty)}$$

This choice of T_* is particularly meaningful when local boundary-layer similarity holds, as in the present problem. For we may then apply Crocco's integral

relation, and the reference temperature T_* given above is seen to be simply an average temperature across the hypersonic boundary layer, i.e.[+]

$$T_* = \int_0^1 T \frac{du}{u_\infty} \approx \int_0^1 T \frac{du}{u_s}$$

The skin friction and the heat-transfer rate on a flat plate under uniform pressure based on T_* of Eq. (2.4) agree exceedingly well with results based on the Young formula[52] in the higher Mach number range, provided the Prandtl number is not far from unity. A comparison of these results, including the results based on T_w as a reference temperature, is given in Table I.

[+] An examination shows that T_* given by Eq. (2.4) turns out to be quite close to the reference temperature proposed by Eckert[51].

SECTION 3

LEADING-EDGE BLUNTNESS EFFECT AND DETACHED SHOCK LAYER

A Model for the Inviscid Flow Field

The necessity of allowing the shock layer to detach from the afterbody of a blunt leading edge is evidenced by the breakdown of the standard shock-layer theory around the shoulder region where the pressure would accordingly fall below zero and the shock-layer thickness would become infinite. The essence of our analysis is that the pressure at the base of the detached layer will not be assumed equal to zero, a priori, as was done for a free layer[39], but is to be determined as part of the solution to the problem.

It is essential to realize that, within the inviscid, hypersonic-flow region bounded by the shock and the body (i.e., the outer edge of the boundary layer) downstream of a small blunt nose, there is an inner core of considerable extent containing gas particles which have come through the comparatively forward, and hence stronger, portion of the shock (see Fig. 1). It is appropriate to term this region an entropy layer, since its specific entropy is much higher than that prevailing near the adjacent shock. The temperature within this layer is accordingly much higher, and the density much lower, than the corresponding values near the shock; the gas within the entropy layer has been heated, so to speak, by the strong forward portion of the curved shock. It is natural to consider the remaining, and relatively thin, high-density part of the flow field behind the shock as a shock layer in the usual sense, except for the fact that it is no longer attached to a rigid body. The equivalent body surface for this shock layer over the relatively slender, downstream portion of the flow field can be taken to coincide with the outer edge of the entropy layer, $y = Y_e(x)$,

which, in view of the particle-isentropic condition, must also be a streamline (see Fig. 1b). Across this streamline boundary, the pressure must be continuous.*

The flow structure within a hypersonic shock layer has been treated quite extensively by Freeman[37] and others[38-40]. Our present study will deal with the entropy layer, the outer edge of which is the base of the shock layer. To do so, we need a knowledge of the pressure at the base of the shock layer in terms of Y_e. The leading approximation under (b) and (c) for this relation, according to shock-layer analysis, is simply

$$p_e \approx \rho_\infty U^2 \left[Y_e'^2 + Y_e Y_e'' \right] \tag{3.1}$$

which represents the Newtonian-plus-centrifugal (Busemann) pressure formula simplified for thin bodies. The corresponding formula in the axisymmetric case is

$$p_e \approx \rho_\infty U^2 \left[Y_e'^2 + \frac{Y_e Y_e''}{2} \right]$$

Restrictions of the Present Analysis

In view of the high temperature attained within the entropy layer, the local velocity u could be considerably reduced from its free-stream value U. Since the assumption of $u_\delta \approx U$ has been made in the boundary-layer analysis, and will be used later in the treatment of the entropy layer, an assessment of the magnitude of $\Delta u/U$ is important and will be made prior to further development.

* It may be noted that in the vicinity of the blunt-nose region, the inner edge of the shock layer (which in this instance is a free layer) may not be closely represented by a streamline. This implies that streamlines within the entropy layer actually come from various points along the curved bow shock upstream (see Fig. 1a), and the distribution of entropy within the entropy layer is not generally uniform. The validity of the assumption that the inner edge of the detached shock layer approaches a streamline depends, in fact, on the small-distance assumption (a).

For the purpose of examining the magnitude of $\Delta u/U$ in the entropy layer, we consider first the particular case of a flat plate under the influence of the strong blast-wave effect produced by its blunt tip. For this case, the surface pressure distribution is quite well established by the consistent results of the blast-wave theory[19,20,24] and the correlated numerical calculations based on the characteristics method[23]. We can therefore determine the maximum value of the perturbation velocity (for arbitrary x) from the particle-isentropic condition and the Bernoulli relation. Maximum values of $|\Delta u/U|$ for γ = 1.20, 1.40, and 1.667 are presented in Fig. 2 as a function of x/kt . The results indicate that sufficiently far downstream of a blunt nose ($x/kt \gtrsim 10$), $\Delta u/U$ remains sufficiently small to permit the approximation $u \approx U$ *.

Since in most cases,

$$p_b < p_s \approx \frac{2\gamma}{\gamma+1} M^2\theta^2$$

where θ is the local shock angle (which gives also the typical local flow angle), a conservative estimate for the perturbation velocity may be obtained from the Bernoulli relation, which can be taken as

$$\left|\frac{\Delta u}{U}\right| \lesssim \frac{1}{2}(\theta)^{2\frac{\gamma-1}{\gamma}}$$

where the exponent $2(\gamma-1)/\gamma$ has the values 1/3, 4/7, and 4/5 for γ = 1.20, 1.40, and 1.667 respectively.

We may now state more explicitly, in terms of the typical flow deflection angle, the requirements which will control the degree of accuracy of the subsequent analysis of the inviscid-flow region, as well as of the boundary layer:

---

* At $x/kt \geq 10$, $|\Delta u/U| \leq$ 0.12, 0.16, and 0.26 for γ = 1.667, 1.40, and 1.20, respectively. In the calculation for γ = 1.20 , the pressure formula given by the zero-order theory for small ϵ has been used.

(A) $\frac{1}{2}(\theta)^{2\frac{\gamma-1}{\gamma}}$ must be <u>negligible</u> in comparison with unity

(B) $1/M^2\theta^2$ must be <u>sufficiently</u> small in comparison with unity

(C) ϵ must be <u>sufficiently</u> small in comparison with unity

Obviously, condition (A) is essential for the assumption $u = U$ at the outer edge of the boundary layer and within the entropy layer as well. Condition (B) calls for a sufficiently strong shock, and (C) and (B) together will permit treatment by the shock-layer concept. By these requirements, the admissible ranges of the shock (and flow) angle θ, and ϵ, are necessarily restricted: To satisfy the small-perturbation assumption, θ must be small, but not so small that the shock cannot remain strong. In addition, the shock-layer approximation requires ϵ to be close to unity, but not so close that the small-perturbation assumption will be violated. The ranges for θ and ϵ can, of course, be enlarged by increasing M and by including (consistently) terms of higher orders in ϵ and $1/M^2\theta^2$.

<u>Analysis of the Entropy Layer</u>

Our analysis will be based on the fact that the density within the entropy layer is low compared to that in the free stream, i.e. $\rho \ll \rho_\infty$. It is essential to examine the compatibility of this fact with the requirements set forth above. Since the density depends not only on the pressure but also on the entropy, we should distinguish two situations. In one, the streamlines over most of, or at least a considerable part of, the entropy layer come from the immediate vicinity of the blunt nose. In other situations, the streamlines from the blunt nose region reach only a small fraction of the entropy layer.*

* The rest of the streamlines in the entropy layer come from the slender but still comparatively forward and stronger portion of the curved bow shock.

In the first situation, the specific entropy is at the same level as that prevailing at the nose, and the order of magnitude of the density may therefore be represented for particle-isentropic flow by

$$\frac{\rho}{\rho_\infty} \approx \frac{\gamma+1}{\gamma-1}\left(\frac{p}{p_N}\right)^{\frac{1}{\gamma}} = O\left[\frac{1}{\epsilon}(\theta)^{\frac{2}{\gamma}}\right]$$

Comparing this with requirement (A), we see that the local density is indeed small in comparison with the free-stream value when (A) is satisfied.* In the second situation, the density distribution given by the strong blast-wave theory[18,19,20,25,26] should be valid, since streamlines over most parts of the entropy layer now come from the slender portion of the shock; hence, the hypersonic small-disturbance theory applies. The fact that the blast-wave solutions reveal the structure of a detached shock layer and a low-density entropy layer is well known. The ratio ρ/ρ_∞ in this situation may, in fact, be represented by (assuming a flat-plate afterbody)

$$\frac{\rho}{\rho_\infty} = O\left[\frac{1}{\epsilon}\, e^{-\frac{1}{\epsilon}}\right]$$

which is small for all practical purposes. The second situation may perhaps be realized only for an extremely small blunt nose (hence large x/t) together with an extremely high Mach number. In either situation, the supposition

$$\frac{\rho}{\rho_\infty} \ll 1 \qquad (3.2)$$

within the entropy layer can be well justified. Its error is presumably no larger than that incurred by the assumption $u \approx U$, that is, requirement (A).

An immediate consequence of the low density in the entropy layer is that the variation of pressure across it is small enough to be negligible. We can examine this from the equation of motion governing the momentum component in the

* Note that under requirement (A), $\theta^{2/\gamma} \ll \epsilon$ for $\epsilon \ll 1$.

direction transverse to the layer. The fractional variation in pressure across the entropy layer is readily seen to be

$$\left| \frac{p - p_e}{p_e} \right| = O\left[\frac{\rho}{\rho_\infty} \left(\frac{Y_e - Y_b}{Y_e} \right) \right] = O\left(\frac{\rho}{\rho_\infty} \right) \ll 1 \qquad (3.3)$$

and is therefore negligible according to our requirements.

In view of the above conclusion, we can now employ the simplification

$$\left.\begin{aligned} u &\approx U \\ p &\approx p_e(x) \end{aligned}\right\} \qquad (3.4)$$

for study of the flow pattern within the entropy layer. The equations stating conservations of mass and entropy are

$$\left.\begin{aligned} \left(u \frac{\partial}{\partial x} + v \frac{\partial}{\partial y} \right) \rho &= -\rho \frac{\partial v}{\partial y} \\ \left(u \frac{\partial}{\partial x} + v \frac{\partial}{\partial y} \right) \ln \rho &= \frac{1}{\gamma} \left(u \frac{\partial}{\partial x} + v \frac{\partial}{\partial y} \right) \ln p \end{aligned}\right\} .$$

Eliminating the density ρ and making use of the simplification on u and p, these two equations give an equation for v, or v/u. This equation can be integrated to yield

$$\frac{v}{u} = Y_b'(x) + \frac{(Y_b - y)}{\gamma} \frac{d}{dx} \ln p_e \qquad (3.5)$$

for which the following boundary condition at the inner edge of the entropy layer (also the outer edge of the boundary layer)

$$v/u = Y_b'(x) \qquad \text{at} \qquad y = Y_b(x)$$

has been satisfied. Putting dy/dx for v/u, we can integrate Eq. (3.5) once again and obtain an equation for the streamline

$$\left[y - Y_b(x)\right]^{\gamma} p_e(x) = m \tag{3.6}$$

where m is a constant differing for each streamline. This equation should hold throughout the entropy layer. Applying it at the streamline boundary, $y = Y_e(x)$, we arrive at

$$\left[Y_e(x) - Y_b(x)\right]^{\gamma} p_e(x) = \text{constant}. \tag{3.7}$$

This simple integral relation between the pressure and the cross-section area of the entropy layer is basic to our subsequent development. The corresponding integral relation in the axisymmetric case is

$$\left[Y_e^2 - Y_b^2\right]^{\gamma} p_e = \text{constant}.$$

The pressure p_e is that at the base of the shock layer, $Y = Y_e$, and is given by shock-layer theory once $Y_e(x)$ is specified. This relation for p_e from shock-layer theory can be used to eliminate p_e in Eq. (3.7), and we can write down, at least in principle, an ordinary differential equation involving only Y_e. The shock-layer theory gives the Busemann formula, Eq. (3.1), as a leading approximation. The pressure-area relation consistent with this approximation is therefore reducible to (from Eq. (3.7)).

$$(Y_e - Y_b)(Y_e Y_e')' = \text{constant}.$$

In carrying out a higher-order analysis (in ϵ and $1/M^2\theta^2$), we should not

only employ a pressure formula correct to the order desired*, but also work consistently with a more accurate pressure-area relation based on Eq. (3.7).

The constant on the right of Eq. (3.7) is necessarily related to the drag of the blunt nose, as a consideration of the balance of momentum in the streamwise direction will readily show. With the help of the equation of continuity and making use of the small-perturbation requirement (A), we can write for $M > 1$ the equation relating drag and momentum flux as

$$\frac{D_N}{2} + \int_{+0}^{x} p_b Y_b' dx = \int_{Y_b}^{Y_s} \frac{p}{\gamma-1} dy + \int_{Y_b}^{Y_s} \frac{\rho w^2}{2} dy - \frac{p_\infty}{\gamma-1} Y_s \qquad (3.8)$$

where D_N is the drag contributed by the pressure distribution around the small blunt nose**. The second term on the left of Eq. (3.8) then represents the drag contributed by the afterbody. The first and the second integrals on the right of Eq. (3.8) may be interpreted, respectively, as the internal and kinetic energies associated with the cross-flow field. As a result of the small-perturbation requirement, the streamwise perturbation velocity u does not enter into the above relation.

In view of the drastic difference in the density between the entropy layer and shock layer, it is convenient to write the second integral on the right of Eq. (3.8) as

---

* The first-order ϵ correction to the Busemann formula has been given explicitly by Freeman in Ref. 37.

** The nose drag D_N has been defined as the total drag of a symmetrical nose, namely, $y = \pm Y_o(x)$. In the case without top-bottom symmetry, $D_N/2$ should then be taken as the contribution of one part of the surface which begins at the apex, or the stagnation point, of the nose.

$$\int_{Y_b}^{Y_e} \frac{\rho v^2}{2}\, dy + \int_{Y_e}^{Y_s} \frac{\rho v^2}{2}\, dy$$

The lateral extent of the shock layer is generally of an order higher than that of the entropy layer, i.e.,

$$(Y_s - Y_e) : (Y_e - Y_b) = O\left[\epsilon + 1/M^2\theta^2\right] : 1$$

whereas the ratio of density in the entropy layer to that in the shock layer is

$$\left[\left(\frac{\rho_e}{\rho_\infty}\right) \cdot (\epsilon + 1/M^2\theta^2)\right]$$

As a result, the magnitude of the first integral is seen to be smaller than that of the second by a factor ρ_e/ρ_∞. To be consistent with Eqs. (3.2) and (3.3), we may omit the first integral in comparison with the second. Now, if only zero and first-order terms are to be retained in the momentum-drag relation, the kinetic-energy integral can, of course, be further simplified, and Eq. (3.8) may be written as

$$\epsilon D_N + 2\epsilon \int_{+0}^{x} p_b Y_b' dx \approx \int_{Y_b}^{Y_s} p\, dy + \epsilon \rho_\infty U^2 Y_e Y_e'^2 - p_\infty Y_s \qquad (3.8a)$$

which is correct to, and includes terms of, the first order of $(\epsilon + 1/M^2\theta^2)$. The afterbody drag integral on the left is of the same order as $p Y_b \epsilon$. Since $p \sim \rho_\infty U^2\theta^2$, the second terms on both sides of the equation, as well as $p_\infty (Y_s - Y_b)$, will be of order $(\epsilon + 1/M^2\theta^2)$ higher than the first integral on the right, and they can all be dropped in the leading approximation. This agrees with the observation that for ϵ small the number of degrees of freedom

excited becomes very large, and most of the energy gained by the flow field appears as internal energy, which is the remaining term on the right.

Since the pressures in the shock and the entropy layers belong to the same order, we can replace the location of the shock by the base of the shock layer in the zero-order approximation, and the momentum relation Eq. (3.8), to this approximation, is reduced therefore to

$$\epsilon D_N = p_e (Y_e - Y_b)$$

That is,

$$(Y_e - Y_b)(Y_e Y_e')' = \epsilon D_N / \rho_\infty U^2 \qquad (3.9)$$

This is the pressure-area relation pertaining to the zero-order theory previously given, but with the constant now determined. For the axisymmetric case, the corresponding relation is

$$\left[Y_e^2 - Y_b^2\right]\left[Y_e'^2 + Y_e Y_e''/2\right] = 2\epsilon D_N / \pi \rho_\infty U^2 .$$

For the zero-order approximation, it seems that consideration of the momentum-integral relation not only determines the constant of Eq. (3.7), but also furnishes an alternative, and apparently simpler, derivation of the pressure-area relation. For the higher approximation, however, we may find it convenient to use Eq. (3.8) strictly as a subsidiary condition. The constant in the pressure-area relation, Eq. (3.7), can be determined by passing to the limit $\psi \longrightarrow +0$ in Eq. (3.8).

We may note that, on the basis of Eq. (3.9), the pressure p_e, i.e., $(Y_e Y_e')'$, can never become negative. This is to be expected since the shock

layer in our treatment is no longer required to follow the body surface. However, Eq. (3.9), as well as Eq. (3.7), has not excluded the possibility of an attached shock-layer, and also contains the free layer as a limiting solution. We can see this readily by examining Eq. (3.9) for the nearly limiting situation of an extremely small nose. The constant on the right of Eq. (3.9) in this case then reduces to a very small but positive number. Now, for p_e to be finite, it is clear that the shock layer must remain essentially attached to the body, i.e., $Y_e \approx Y_b$. As soon as p_e approaches zero, the entropy layer will, accordingly, begin to thicken and the shock layer will detach to form a free layer.

Discussion

On the basis of the foregoing analysis, the fields of pressure and velocity, as well as the locations of the shock can all be consistently determined under requirements (A)-(C). We have arrived at these results without the need of simultaneously knowing the density distribution within the entropy layer, except for the fact that the density level of the entropy layer is comparatively low. On the other hand, the present theory actually affords no solution for the entropy field; to find the density or entropy in the entropy layer, certain detailed knowledge of the flow field around the blunt-nose region would be necessary. It must, however, be pointed out that the determination of density may no longer be a trivial matter for the present problem if the assumption of constant specific heats were removed. For, under this more general situation, the value of density would be essential for determining the local thermodynamic properties, hence the local value of ϵ, which in turn will determine the pressure and velocity fields. In this case, it will be more appropriate to redefine ϵ as $\epsilon \equiv p/2\rho h$ and the relation corresponding to Eq. (3.9) becomes (ν = 0, or 1),

$$p_e(x)\int_{Y_b}^{Y_e}\frac{(\pi y)^\nu\,dy}{\epsilon(x,y)} = D_N$$

The results of the above analysis confirm, in a certain sense, the validity of the blast-wave theory for the tip-bluntness problem[18-20]. In spite of the fact that the blast-wave theory of Refs. 18, 19 and 20 does not take proper account of the presence of the entropy layer, and gives erroneous values for the entropy and density near the body surface, the pressure and velocity determined by the present analysis of the entropy layer may be identified as those of the blast-wave theory, as an inspection of the governing Eqs. (3.7) and (3.8) will readily reveal.

Our general approach to the inviscid leading-edge problem is also similar to a treatment given previously by Chernyi[21,22], as pointed out earlier. In Chernyi's treatment, which is essentially a momentum-integral method, use is made of $u \approx U$ and $p \approx p_e(x)$. The basic equations employed, written here for steady plane flows, are

$$\left.\begin{aligned}\frac{D_N}{2}+\int_{+0}^{x}p_b\,Y_b'\,dx &= \frac{p_b}{\gamma-1}(Y_s-Y_b)+\frac{\rho_\infty}{2}U^2Y_s(Y_s')^2\\ p_b &= \rho_\infty U^2\left(Y_s'^2+Y_sY_s''\right)\end{aligned}\right\}\qquad(3.10)$$

We note that the first of Eq. (3.10), except for the first term on the right-hand side, is almost the same as Eq. (3.8a). It is evident that, as far as the leading approximation for small ϵ and $1/M^2\theta^2$ is concerned, the above equation and Eq. (3.9) obtained by the present study are essentially equivalent. When the higher-order approximations are considered, we must compare Chernyi's equation, i.e., Eq. (3.10), with our Eq. (3.7). We may note that, implicitly in

Eq. (3.10), the outer edge of the entropy layer has been replaced by the shock itself, and the Busemann pressure formula has been used. Hence, it is doubtful that Eq. (3.10) would yield a consistent correction to the leading approximation. At any rate, the two treatments are seen to be quite different when higher-order approximation is considered.

The entropy layer downstream of a blunt nose has also been studied recently by Guiraud[42,43]. By an ingenious mathematical technique on which the writer is not in the position to elaborate, Guiraud has arrived at an equation which can be readily identified as the pressure-area relation, Eq. (3.7), given above. However, Guiraud does not use the momentum-drag relation, Eq. (3.8) or Eq. (3.8a), to determine the constant term on the right of Eq. (3.7). Instead, he relates the term to an integral involving shock curvature in the nose region. Hence, this term cannot be explicitly determined until the complete problem involving the nose region is solved. Strictly speaking, therefore, the results of Guiraud's study in Refs. 42 and 43 do not fall into the same class as the blast-wave theory.

The reason for the departure of Guiraud's treatment from the present one at the final stage of the analysis may be related to the remarks given in Ref. 42: There, Guiraud observed that, for a flat-plate afterbody, Eq. (3.7) calls for $p_e \propto Y_e^{-\gamma}$. If one assumes $Y_e \propto Y_s$, then

$$p_e \propto \left(\frac{d Y_e}{dx}\right)^2 \propto \frac{Y_e^2}{x^2} ,$$

and hence,

$$Y_e \propto x^{\frac{2}{2+\gamma}} ;$$

whereas the blast-wave theory provides $Y_s \propto x^{2/3}$. It was thus concluded that the momentum-drag integral relation which leads to the blast-wave result cannot be used to determine the constant since it appears to contradict the pressure-area relation, Eq. (3.7), unless $\gamma \longrightarrow 1$. It must be noted, however, that no streamline in a self-similar hypersonic flow field, except for those on the body, can be similar to the shock surface, i.e., $Y_e \propto Y_s$ cannot be true. Otherwise, there could be no flow into the region between the shock and the body. In fact, Eq. (3.7) states just this fact. For, according to the blast-wave results, $Y_s \propto x^{2/3}$ and $p_e \propto p_s \propto (Y_s/x)^2 \propto x^{-2/3}$; the streamline boundary for the entropy layer will then be given by the pressure-area relation as

$$Y_e \propto p_e^{-1/\gamma} \propto x^{2/3\gamma} \quad (\neq x^{2/3})$$

The consistency between $Y_s \propto x^{2/3}$ and $Y_e \propto x^{2/3\gamma}$ for small but nonvanishing ϵ can indeed be checked by the results of the higher-order analysis of the shock-layer theory[37].

Implicit in the foregoing discussion is the assumption that the physically meaningful solution to Eq. (3.7), when the leading-edge effect predominates, is the blast-wave solution $Y_s \propto x^{2/3}$. The fact that the blast-wave solution does not necessarily represent the complete solution to Eq. (3.7) can be seen by examining the corresponding equation for small ϵ in the case of the flat-plate afterbody, that is,

$$Y_e \left(Y_e Y_e' \right)' = \epsilon \, D_N / \rho_\infty U^2$$

The complete solution of this equation can be readily found.* However, the only particular solution which is compatible with the small-disturbance requirement turns out to be $Y_s \propto x^{2/3}$. A detailed discussion of this point is given in Appendix I. For reasons of consistency, the solution to Eqs. (3.7) or (3.9) when bluntness dominates will be taken to be $Y_s \propto x^{2/3}$ throughout the present analysis.

In what follows, we shall apply the results of the above analysis to the problem involving both tip bluntness and boundary-layer displacement effects. The zero-order theory for small ϵ and large $M^2\theta^2$ will be developed in detail.

* The existence of a complete solution, in this case, was called to the writer's attention by Mr. J. P. Guiraud in a recent communication.

SECTION 4

THE ZERO-ORDER THEORY FOR INTERACTION OF THE BOUNDARY LAYER AND ITS OUTER FLOW UNDER THE INFLUENCE OF LEADING-EDGE BLUNTNESS

The Governing Equations for Small ϵ and Large $M^2\theta^2$

For small ϵ, the boundary layer has been shown to be governed by local similarity, and assuming, in addition, the shock wave involved is strong, the simple pressure-area relation Eq. (3.9) from the analysis of the entropy layer should also hold. Combining these results, the leading-edge problem of hypersonic flows subject to the tip bluntness and boundary-layer displacement effects can be treated in a rather straightforward fashion.

To apply Eq. (3.9) to this problem, the inner edge of the entropy layer, $Y_b(x)$, will be taken as an equivalent body surface which should account for the displacement effect of the hypersonic boundary layer. Inasmuch as the assumption $u_\delta \approx U$ is valid[5,7], the outer edge of the boundary layer may be approximately represented by the displacement thickness δ_* because of the extreme low density resulting from viscous heating. In this instance, we can replace Y_b by $Y_w(x) + \delta_*(x)$. By local similarity, δ_* is given by Eq. (2.3) explicitly in terms of the pressure distribution, which is now provided by the Busemann formula.

The equation governing the zero-order approximation, that is, the leading approximation for small ϵ and large $M^2\theta^2$, is, for the plane flow,

$$\left.\begin{aligned} &\left[Y_e - Y_w - \delta_*\right]\left(Y_e Y_e'\right)' = \epsilon k\, t/2 \\ &\delta_* = \epsilon\left(0.664 + 1.73\,\frac{T_w}{T_o}\right)\frac{\bar{\pi}_L\sqrt{L}}{M^2}\,\frac{\sqrt{Y_e Y_e'}}{\left(Y_e Y_e'\right)'} \end{aligned}\right\} \qquad (4.1)$$

After solving Eq. (4.1) for Y_e , we can determine the pressure from the Busemann formula and the heat-transfer rate as well as the skin friction from Eq. (2.3). The rudimentary manner in which the three flow regions -- boundary layer, entropy layer, and shock layer -- interact is contained in the ordinary differential equation given above. In the absence of tip bluntness, we have only the shock layer and the boundary layer. The first of the above equations then becomes

$$Y_e = Y_w + \delta_*$$

and Eq. (4.1) reduces to

$$2(Y_e - Y_w)\left[\sqrt{Y_e Y_e'}\right]' = \epsilon\left(0.664 + 1.73\,\frac{T_w}{T_o}\right)\frac{\bar{\tau}_L\sqrt{L}}{M^2} \qquad (4.1a)$$

Near the origin, $x = +0$, Eq. (4.1) admits the singular solution $Y_e \sim x^{2/3}$*. This is the correct behavior when the blast-wave effect of the leading edge is strong[19,20], and confirms that near the leading edge the displacement effect of the boundary layer gives way to the more powerful effect of leading-edge bluntness. For cases which do not involve bluntness, Eq. (4.1a) reveals singular behavior of another type: as $x \to 0$, $Y_e \sim x^{3/4}$* . This is the behavior to be expected when the displacement effect predominates[5,6,9]. With these singular solutions as leading terms, solutions to Eq. (4.1) can be obtained by a forward integration from the origin. These asymptotic solutions for Y_e , as well as the pressure and the heat transfer, will be examined subsequently for flat-plate afterbodies.

---

* For Eq. (4.1), we shall assume that as $x \to 0$, $Y_w \sim x^{\sigma}$, where $\sigma > 2/3$. For Eq. (4.1a), we assume that as $x \to 0$, $Y_w \sim x^{\sigma}$, where $\sigma > 3/4$. In any case, assuming a regular afterbody shape, i.e., $Y_w \sim x$ as $x \to +0$, will be sufficient.

As is obvious from the requirements (A)-(C), the error in the zero-order theory is presumably of the order

$$O\left[\epsilon + \frac{1}{M^2\theta^2} + \frac{1}{2}(\theta)^{2\frac{\gamma-1}{\gamma}}\right] .$$

If terms of the next orders are consistently included in the analyses of the entropy layer and of the boundary layer, in the manner previously described, the first two error terms may presumably reduce to ϵ^2 and $1/M^4\theta^4$.

In view of their frequent occurrence in the later development, it is convenient to introduce two new variables for the plane flow,

$$K_\epsilon \equiv M^3 \epsilon k \frac{t}{x}$$

$$\tau_\epsilon \equiv \epsilon\left(0.664 + 1.73\,\frac{T_w}{T_0}\right) M^3 \sqrt{\frac{C}{Re}} \qquad (4.2)$$

where

$$Re \equiv \frac{\rho_\infty U x}{\mu_\infty}$$

Except for the factors ϵ and $\epsilon\,(0.664 + 1.73\,T_w/T_0)$, these two variables are those employed previously for the bluntness and the displacement problems[1-24].

In what follows, the zero-order theory will be applied to the problem of a flat plate in hypersonic flow subject to the three effects of bluntness, displacement, and angle of attack. In order to see clearly the manner in which these effects will act in combination, the simpler problems involving only two simultaneous effects (namely, $K_\epsilon - \tau_\epsilon$, $\tau_\epsilon - M\alpha$, $K_\epsilon - M\alpha$) will first be singled out for discussion.

The Flat Plate with Bluntness and Displacement

For this problem, Eq. (4.1) can be reduced to

$$z\,(z\,z')' - \sqrt{z\,z'} = 1 \qquad (4.3)$$

where the new variables are

$$z = 8M\left[\gamma_\epsilon^2 / K_\epsilon\right] Y_e / K_\epsilon \varkappa$$

$$\zeta = 16\left[\gamma_\epsilon / K_\epsilon^{2/3}\right]$$

Note that both $K_\epsilon \varkappa\,(= M^3 \epsilon k t)$ and $\gamma_\epsilon^2 / K_\epsilon \left[= \epsilon \left(0.664 + 1.73 \frac{T_w}{T_o}\right)^2 M^3 C / k Re_t\right]$ are independent of $\varkappa$. Therefore, z and ζ are proportional, respectively, to Y_e and $\varkappa$. Let $\phi = z^2/2$ and $\lambda = d\phi/d\zeta$. Equation (4.3) may then be written

$$\sqrt{2\phi}\ \lambda\ d\lambda/d\phi - \sqrt{\lambda} = 1$$

which can be integrated by a separation of variables to give

$$\phi = 4\left[\sqrt{\lambda} - \lambda/2 + \lambda^{3/2}/3 - \ln(1+\sqrt{\lambda})\right]^2$$

This result provides the desired behavior at the origin, namely $Y_e \sim \varkappa^{2/3}$ as $\varkappa \longrightarrow 0$. To obtain a relation between ζ and ϕ, we note that

$$d\zeta = \frac{d\zeta}{d\phi}\, d\phi = \frac{1}{\lambda}\,\frac{d\phi}{d\lambda}\, d\lambda$$

and the solution of Eq. (4.3) can finally be brought to the parametric form

$$\left.\begin{aligned} z &= 2\sqrt{2}\left[\sqrt{\lambda} - \lambda/2 + \lambda\sqrt{\lambda}/3 - \ln(1+\sqrt{\lambda})\right] \\ \zeta &= (1+\sqrt{\lambda})^4 - \frac{22}{9}(1+\sqrt{\lambda})^3 + 9(1+\sqrt{\lambda})^2 - \frac{46}{3}(1+\sqrt{\lambda}) \\ &\quad + \frac{10}{3}\ln(1+\sqrt{\lambda}) - 4\sqrt{\lambda}\ln(1+\sqrt{\lambda}) + 2\left[\ln(1+\sqrt{\lambda})\right]^2 + \frac{76}{9} \end{aligned}\right\} \qquad (4.4)$$

This result for Y_e , which may also be taken as the shock location Y_s , is presented in Fig. 3(a) as $M\left[\chi_\epsilon^2/K_\epsilon\right]^2 Y_e/K_\epsilon \nu$ vs. $\chi_\epsilon/K_\epsilon^{2/3}$. The corresponding surface pressure and the surface heat-transfer rate are given in (b) and (c) of the same figure as $\left[K_\epsilon/\chi_\epsilon^2\right]^2 p_w/\gamma_\infty p_\infty$ and $\epsilon\left(0.664 + 1.73\,\frac{T_w}{T_0}\right)\times \left[K_\epsilon/\chi_\epsilon^2\right]^2 M^3 c_H/\sqrt{\gamma_\infty}$. We can see that Y_e varies as $\chi^{3/4}$ as $\chi \longrightarrow \infty$, and as $\chi^{2/3}$ as $\chi \longrightarrow 0$. These two limits correspond to situations in which displacement and bluntness dominate, respectively, agreeing with strong-interaction theory in the first case and strong blast-wave theory in the second. One important feature here is that all parameters and spatial variables are grouped together to form one single variable $\chi_\epsilon/K_\epsilon^{2/3}$. From Fig. 3 we see that transition from the strong blast-wave to the strong-interaction regimes occurs in the range

$$10^{-1} < \chi_\epsilon/K_\epsilon^{2/3} < 2$$

A variable analogous to $\chi_\epsilon K_\epsilon^{-2/3}$, which controls the combined effect of bluntness and displacement, has been previously pointed out by Lees and Kubota in a discussion assuming a weak nose effect[2].

The appearance of γ_∞ and $\sqrt{\gamma_\infty}$ in the nondimensional forms of pressure and heat-transfer rate introduced above result from the use of the Busemann formula

$$p_e/\rho_\infty U^2 = p_e/\gamma_\infty p_\infty M^2 = \left[Y_e'^2 + Y_e Y_e''\right]$$

Retaining the factor γ_∞ , instead of replacing it by unity, is in keeping with the convention of existing shock-layer theories[35-40]. Furthermore, it permits ϵ to represent conditions behind the shock even when ϵ_∞ is not small.

It is of interest to examine more closely the asymptotic solutions. They can be written, for large and small $\left[\chi_\epsilon / K_\epsilon^{2/3}\right]$, respectively, as

$$\left.\begin{aligned} M Y_s / x &= 1.21\sqrt{\chi_\epsilon}\ , && 1.31 (K_\epsilon)^{1/3} \\ p_w / \gamma_\infty p_\infty &= \frac{\sqrt{3}}{2}\chi_\epsilon\ , && \left(\frac{1}{18}\right)^{1/3}(K_\epsilon)^{2/3} \\ \epsilon\left(0.664 + 1.73\frac{T_w}{T_0}\right) M^3 c_H / \sqrt{\gamma_\infty}\ \chi_\epsilon &= 0.219\sqrt{\chi_\epsilon}\ , && 0.119 (K_\epsilon)^{1/3} \end{aligned}\right\} \quad (4.5)$$

The appearance of χ_ϵ in the above strong-interaction solutions indicates clearly the roles of ϵ and the wall temperature level. In view of the factor $(0.664 + 1.73\, T_w/T_0)$ in χ_ϵ, the boundary-layer displacement effect will depend strongly on the wall temperature. An interesting observation is that if we simply add the two asymptotic solutions for p_w/p_∞, the sum differs from the exact solution in the transition region by less than 12%. This seems to lend support to the empirical linear-combination laws proposed previously by certain investigators[29-31], at least when ϵ is small.

We may now compare the zero-order solution in the two limits with the corresponding self-similar solutions which do not assume γ close to unity. In Tables II and III, results from a few of these existing solutions[6,17,20,24,26] for $\gamma = 1.40$ are tabulated and compared with those of Eq. (4.5). Some of these results are also shown in Fig. 3. We may conclude from these comparisons that as an approximation for the surface pressure and skin friction when $\gamma = 1.4$, the present zero-order solution may not be adequate, and a higher-order solution (in ϵ) appears desirable. For the surface heat-transfer rate as well as the shock shape, however, the zero-order theory works reasonably well, in spite of the fact that γ in this case is actually not too close to unity.

The Inclined Flat Plate with Boundary-Layer Displacement

With bluntness excluded, Eq. (4.1a) can be transformed to

$$(z \mp \zeta)(\sqrt{z}\,\bar{z})' = 1 \tag{4.6}$$

where the variable z and ζ now stand for

$$\left.\begin{aligned} z &= 4M^4|\alpha|^3\, Y_e/\chi_\epsilon^2 x \\ \zeta &= 4\left[M^2\alpha^2/\chi_\epsilon\right]^2 \end{aligned}\right\}$$

The angle of attack of the plate, α, is positive for compressive flow over the plate. The negative sign in front of ζ in Eq. (4.6) applies to $\alpha > 0$. In view of the strong shock requirement, our solution for $\alpha < 0$ pertains only to the situation when the boundary layer is thick enough to induce a strong bow shock. This implies that the region of validity is confined to certain upstream portions of the flow field, and to a rather small range of negative α. Again, there is only one variable governing the problem. In this case, it is $M^2\alpha^2/\chi_\epsilon$. Equation (4.6) appears to be quite different from that underlying the analysis of Pai and Shen[1,7,10]. The difference presumably arises from the use of a different formula for the pressure.

For the case of $\alpha > 0$ the asymptotic solution of Eq. (4.6) for large $M^2\alpha^2/\chi_\epsilon$, i.e., large x, is simply that for a wedge without displacement effect, i.e.

$$\left.\begin{aligned} Y_s &= \alpha x \\ p_w/\gamma_\infty p_\infty &= M^2\alpha^2 \\ \epsilon\left(0.664 + 1.73\,\frac{T_w}{T_0}\right) c_H/\sqrt{\gamma_\infty}\,\chi_\epsilon &= \alpha/M^2 \end{aligned}\right\} \tag{4.7}$$

For small argument of the variable, the strong-interaction solution results, as given previously in Eq. (4.5). When the wedge angle is sufficiently small, or $\varkappa$ small, the incidence effect amounts to only a small perturbation on this solution. We may then write Y_e or Y_s as

$$Y_s \approx \frac{2}{(3)^{1/4}} \sqrt{\chi_\epsilon}\, \frac{x}{M} + \frac{3}{10} \alpha \varkappa \qquad (4.8)$$

This development near the sharp leading edge is valid for both $\alpha > 0$ and $\alpha < 0$, and reveals a pattern of asymmetry. The curves for $\alpha > 0$ presented in Fig. 4* give a smooth transition from the regime of strong interaction to that of a usual hypersonic wedge flow. Curves for $\alpha < 0$ in the same figure show a gradual deviation from the Stewartson-Lees solution as we go downstream. For the shock shape and the pressure, the range of transition for $\alpha > 0$ appears to occur in

$$10^{-2} < M^2\alpha^2/\chi_\epsilon < 10$$

whereas for the heat-transfer rate, the value corresponding to the pure wedge-flow solution is closely approached as early as $M^2\alpha^2/\chi_\epsilon = 2$. From the agreement of our zero-order solutions with the self-similar solution for $\gamma = 1.40$ in the two limits (see Fig. 4), we may anticipate the zero-order results to be reasonable for heat transfer, pressure, and shock shape, provided the surface temperature is substantially lower than the stagnation temperature.

---

* The numerical results of Fig. 4 were obtained by digital-machine computation (IBM 704), using an interval of 100 points per unit of $(\zeta)^{1/4}$.

The Inclined Flat Plate with Tip Bluntness and the Corresponding Problem of a Blunted Cone

For the inviscid problem of the blunted flat plate at incidence with negligible boundary-layer displacement effect, we have from Eq. (4.1) the simple differential equation

$$(Z \mp \zeta)(Z Z')' = 1 \tag{4.9}$$

where the variables Z and ζ now stand for

$$\left.\begin{aligned} Z &= 2\alpha^2 Y_e / \epsilon k t \\ \zeta &= 2|\alpha|^3 x / \epsilon k t \end{aligned}\right\}$$

In this case, we again use the same convention for α .

For the purpose of later discussion, we will examine in detail the asymptotic behavior of the solution of this inviscid problem for small and large ζ . Near the leading edge, we find from Eq. (4.9) the desirable result

$$Y_e / t \approx \left(\frac{3}{2}\right)^{2/3} (\epsilon k)^{1/3} \left(\frac{x}{t}\right)^{2/3} + \frac{1}{6}\alpha \left(\frac{x}{t}\right) \tag{4.10}$$

which holds for both positive and negative α and reveals an asymmetrical perturbation of the blast-wave solution. At the far downstream end, where the effect of the surface incidence dominates, we will develop the asymptotic solution only for $\alpha > 0$. Equation (4.9) then yields for large ζ

$$Z \approx \zeta + 1 + \frac{1}{\sqrt{\zeta}}\left[A J_0(2\sqrt{\zeta}) + B Y_\sigma(2\sqrt{\zeta})\right] \tag{4.11}$$

where A and B are constants, and J_σ and Y_σ are Bessel functions of the first and second kind of certain order σ . In view of the first and second terms we see that the shock will tend to the wedge surface, but never quite reach

it, as we go downstream. Most interesting is the oscillatory behavior of the solution. According to the asymptotic behavior of the Bessel functions, the third group of terms of Eq. (4.10) is equivalent to

$$\frac{A}{(\zeta)^{3/4}} \cos(2\sqrt{\zeta} + B)$$

The corresponding behavior of the pressure is then

$$p_w / \gamma_\infty p_\infty M^2 \alpha^2 = (\bar{z}\bar{z}')' \approx 1 - \frac{A}{(\zeta)^{3/4}} \cos(2\sqrt{\zeta} + B) \qquad (4.12)$$

Evident from Eqs. (4.11) and (4.12), this oscillatory decay of the tip-bluntness effect will be more readily revealed in the pressure distribution than in the shock shape. The results obtained from numerical integration of Eq. (4.9) by digital machine computation* are presented (as the full curves) in Fig. 5. The oscillatory decay of the tip-bluntness effect is indeed exhibited by the pressure distribution for $\alpha > 0$.

It may be of interest to point out, in this connection, that the solution to Eq. (4.9) can be approximated surprisingly well by the equation

$$\frac{1}{\bar{z} - \zeta} = (\bar{z}\bar{z}')' = 1 + \frac{1}{\sqrt{\zeta}}\left[0.59\, J_{1/3}(2\sqrt{\zeta}) - 0.71\, Y_{1/3}(2\sqrt{\zeta})\right] \qquad (4.12a)$$

which is also included (as dotted curves) in Fig. 5. The function $\bar{z}$ given above not only agrees with the asymptotic solution Eq. (4.11) for large ζ , but also has a singularity at $\zeta = 0$ identifiable as that of the blast-wave solution. In addition, it satisfies an integral relation of the differential equa-

---

* An interval of 100 points per unit of $(\zeta)^{1/3}$ was used in the computation. The heat-transfer rate, which is not presented, may be obtained in terms of the pressure from Eq. (2.3).

tion Eq. (4.9), namely*

$$\int_0^\infty \left[\frac{1}{z-\zeta} - 1\right] d\zeta = 1$$

The physical significance of the oscillatory decay observed from the above analysis should, of course, be taken with caution. The result of the zero-order solution in this respect is evidently connected with the passage to the mathematical limit, $\gamma \to 1$. Apparently the oscillation represents a repeated reflection or skipping of the reattaching shock layer as it reaches the vicinity of the surface of a very slender afterbody at infinite Mach number. The phenomenon may hence be interpreted as a form of glancing reimpingement of the shock layer. From the very fact that this oscillation is a decay phenomenon, its detail may probably be substantially altered by higher-order ϵ corrections. For $\gamma = 1.40$, in reality we may not have any oscillation in the pressure decay, since the amplitude of the fluctuation shown is never large.

For the purpose of comparing the afterbody effects in two and three dimensions, the results of a similar analysis applied to a blunted slender cone will be briefly discussed. The basic differential equation corresponding to Eq. (4.9) for this axisymmetric problem is

$$(z^2 - \zeta^2)\left(z'^2 + z\,z''/2\right) = 1$$

with

$$\left.\begin{aligned} z &= 2\alpha\gamma_e/\sqrt{\epsilon k}\; t \\ \zeta &= 2\alpha^2\kappa/\sqrt{\epsilon k}\; t \end{aligned}\right\} = \frac{K\alpha^2}{R_N}\,\frac{1}{\sqrt{\epsilon k_2}}$$

* This approximate analytic representation of the solution to Eq. (4.9) was pointed out to the author by Professor H. Pollard of Cornell University.

where α now stands for the half-cone angle, t the nose diameter, and k the nose drag coefficient

$$k \equiv \frac{D_N}{\frac{1}{2}\rho_\infty U^2 \pi t^2/4}$$

The peculiar manner in which the shock layer approaches the afterbody is more markedly revealed in this case than in the case of the blunted wedge. From the results for shock shape presented in Fig. 6(a), we see that the changeover in the vicinity of $\alpha^2 \varkappa / \sqrt{\epsilon k}\, t = 1$ occurs rapidly, as if the detached shock layer remains essentially unaware of the presence of the afterbody until reaching the immediate neighborhood of the cone surface. On the other hand, the corresponding surface pressure, as well as the surface heat-transfer rate (calculated on the basis of local similarity for the laminar boundary layer), given in (b) and (c) of the same figure show a much earlier influence of the afterbody. The oscillation in pressure, decaying as a Bessel function, is again found, but in a rather manifested way. We should note that in this axisymmetric case, the first pressure undershoot, and the oscillatory cycle immediately following it are so pronounced that their occurrence may not be too surprising even when ϵ is not as small, and the shock not as strong, as required by the zero-order approximation. This peculiar behavior of the pressure distribution may be quite meaningful for studies of the influence of bluntness on boundary-layer instability. The pressure undershoot has, in fact, been observed experimentally for slender blunted cones at $M = 6.85$ in air[53].

The undershoot of cone pressure has been predicted previously by Chernyi[5,22], using an integral method discussed in Section 2. For the inviscid flow past a blunted cone with $\gamma = 1.40$, Chernyi finds a strong overshoot following the pres-

sure undershoot. The Bessel function decay is, nevertheless, not found. In a similar treatment for the blunted wedge[21], there is no pressure undershoot, according to Chernyi's result. The difference between the present solutions and Chernyi's presumably results from the difference between Eqs. (3.9) and (3.10).

The Combined Effect of Bluntness, Displacement and Body Thickness

For the flat-plate problem involving all three effects (χ_ϵ, K_ϵ, and $M_\infty \alpha$), we find that a new parameter appears in the reduced form of the solution. If we choose to use, for example,

$$\bar{z} = 8M\left[\chi_\epsilon^2 / K_\epsilon\right]^2 Y_e / (K_\epsilon x)$$

$$\zeta = 16\left[\chi_\epsilon^2 / K_\epsilon^{2/3}\right]^6$$

Eq. (4.1) for this problem becomes

$$(\bar{z} - \Gamma\zeta)(\bar{z}\bar{z}')' - \sqrt{\bar{z}\bar{z}'} = 1 \tag{4.13}$$

where Γ is a parameter (independent of x) given, for the wedge flows, as

$$\Gamma \equiv \frac{K_\epsilon M\alpha}{2\chi_\epsilon^2} \tag{4.14}$$

Figure 7 gives the results of integration for the surface heat-transfer rate in the same variables as used for the zero-incidence case, i.e., Fig. 3(c). Shown are curves corresponding to five positive values of Γ, namely, $\Gamma = 0$, 10^{-2}, 10^{-1}, 1, and 10. The curve for $\Gamma = 0$ has been previously given in Fig. 3(c). Similar calculations may also be carried out for negative values of Γ.

From these results we can see the role of the wedge angle in modifying and controlling the combined effect of the bluntness and boundary-layer displacement.

The slight oscillatory mode revealed in the curve at the upper left corner of Fig. 7 for $\Gamma = 10$ corresponds to the oscillatory pressure behavior discussed previously for the inviscid wedge problem. The results show that when Γ is not too large, the oscillatory phenomenon will subside as a result of the inviscid-viscous interaction.

Hypersonic Similitude Based on the Zero-Order Theory

From the flat-plate problem, we see that the zero-order solution is reducible to a function involving only one variable and the parameter Γ. Viscous hypersonic flows over a blunted inclined plate will accordingly be similar for the same Γ. For thin bodies other than flat plates, we have from Eq. (4.1) the following similitude involving tip-bluntness and boundary layer: For similar bodies generated from the same equation

$$Y_w/\tau L = f\left(\frac{x}{L}\right)$$

the following correlation applies:

$$\left.\begin{array}{l} M\left[\chi_\epsilon^2/K_\epsilon\right]^2 Y_s/K_\epsilon x \\ \left[K_\epsilon/\chi_\epsilon^2\right]^2 p_w/\gamma_\infty p_\infty \\ \epsilon\left(0.664 + 1.73\,\frac{T_w}{T_0}\right)\left[\frac{K_\epsilon}{\chi_\epsilon^2}\right]^3 M^3 c_H/\sqrt{\gamma_\infty} \end{array}\right\} = f\left[\frac{x}{L}; \left(\frac{\chi_\epsilon}{K_\epsilon^{2/3}}\right)_L, \Gamma\right] \qquad (4.15)$$

where f represents the functional dependence concerned. Two alternative forms of Eq. (4.15) can be found in Appendix I.

It is essential to realize that the above correlations do not imply the possibility of obtaining the full similitude for the entire flow field, which should then include the density and temperature fields within the entropy layer. The latter flow quantities in the entropy layers have been excluded from the

present framework of study, however. These correlations based on the zero-order theory, Eq. (4.15), will be subject to the same errors as Eq. (4.1), i.e.

$$O\left[(\gamma-1)+1/M^2\theta^2+\frac{1}{2}(\theta)^{2\frac{\gamma-1}{\gamma}}\right]$$

The most serious among these is presumably that associated with γ. Implicit in the above results are also the assumptions of the linear viscosity-temperature relation, unit Prandtl number, as well as uniform T_w/T_o. Thus for a more accurate correlation under more general conditions, the similitude based on our zero-order theory may not suffice. As a part of the study complementing the foregoing analysis, an examination of the hypersonic similitude under less restrictive conditions will be given in Section 5.

SECTION 5

THE VISCOUS HYPERSONIC SIMILITUDE INVOLVING LEADING-EDGE BLUNTNESS*

For both experimental investigations and practical applications, laws of similitude for correlating flow-field properties under different free-stream conditions and body dimensions are desirable. The similitude arrived at previously in Eq. (4.15) is simple but restrictive. In the following, the more general viscosity-temperature relation $\mu \propto T^{\omega}$ is assumed, the Prandtl number is taken constant but otherwise arbitrary, and the body surface temperature is arbitrary. A perfect gas with constant specific heats is still employed but the specific heat ratio is no longer required to be close to unity.

The inviscid hypersonic similitude which takes into account the effect of slight blunting has been given by the author[54]. In a recent paper, Hayes and Probstein[55] consider the similitude of hypersonic boundary layers. From these two studies a viscous hypersonic similitude involving bluntness is not difficult to infer. Hayes and Probstein caution, however, that the similitude involving bluntness may not be extended to the viscous case, or only under a condition so restrictive as to make the result uninteresting. In view of this, an examination of the basic requirements which underlie hypersonic similitude seems proper at this point.

Basic Requirements for the Validity of Hypersonic Boundary-Layer Similitude Involving Tip Bluntness

Hayes and Probstein observe that the hypersonic small-disturbance theory necessarily fails in the vicinity of the blunt nose itself, and it would appear

* A certain part of the study presented in this Section is based on unpublished work on the subject which was sponsored by the U. S. Air Force Office of Scientific Research (Mechanics Division).

that the theory, hence the "equivalence principle" deduced from it, would break down in the layer of fluid of increased entropy nearest the body. It may then follow that hypersonic similitude cannot hold within the entropy layer as well as the boundary layer beneath it. The major conclusion of our following discussion is that a full similitude capable of correlating the density and temperature distributions near the outer edge of the boundary layer is not possible, but correlations for the pressure and velocity fields, as well as the density and temperature distribution within the boundary layers proper, do exist.

Let us first examine whether similitude can exist in the inviscid flow region. On the basis of our discussion in the earlier part of Section 3, we see that under requirement (A), the approximation $u \approx U$ holds throughout the inviscid flow region including the entropy layer. The applicability of the requirement (A), and the degree of approximation involved, has been examined. From the fact that $u \approx U$ we can conclude that the pressure p and the velocities v and u do obey the equivalence principle, and hence the hypersonic similitude[33]. For the density and temperature in the entropy layer, however, the "equivalence principle" may not be strictly applicable since these quantities may depend on the entropy determined upstream at the nose shock.

For the boundary layer, we observe that, with the wall conditions specified, the solution will be completely determined, by the three quantities at its outer edge: the pressure p_δ, the total enthalpy $H_\delta (= H_\infty)$, and the velocity u_δ. To be sure, for determination of the boundary-layer solution, the specific knowledge of flow density or temperature at the outer edge is actually not necessary. Following essentially the same procedure as Hayes and Probstein in examining the system of equations governing the boundary layer, we find that the

condition required for the existence of boundary-layer similitude is that the quantities p_δ , H_δ and u_δ must obey the equivalence principle in the outer flow. But, under requirement (A), and for M large, this condition can indeed be satisfied. In particular, we have $u_\delta \approx U$. A similitude can therefore exist in the hypersonic boundary layer. We may note that the actual magnitude of the error in the heat-transfer rate, the skin friction, and the displacement thickness incurred by the approximation $u_\delta \approx U$ will not differ a great deal from $\left|\Delta u_\delta / U\right|$. In fact, if we assume local similarity (which is appropriate for the present application) the corrections to these quantities will be, respectively, -1/2, -3/2 and +1/2 of $\left|\Delta u_\delta / U\right|$.

We may hence conclude that, for a perfect gas with constant specific heats and a viscosity-temperature relation $\mu \propto T^\omega$, with the exception of the distributions of density and temperature in the outer flow, the classical hypersonic similitude of Tsien and Hayes can be extended to the boundary layer, even under the influence of the leading-edge bluntness, provided the flow regions immediately downstream of the leading edge are excluded and the flow Mach number is sufficiently high, i.e.

$$\frac{1}{2}(\theta)^{2\frac{\gamma-1}{\gamma}} \ll 1 \qquad M \gg 1$$

When the bluntness effect is not present, the requirement will presumably be less stringent.

The tip-bluntness effect introduces an additional parameter $M^3 k \frac{t}{x}$ into the boundary-layer similitude discussed in Ref. 55. The similarity laws correlating shock shape, surface pressure, surface heat-transfer rate, and skin friction in plane flows may be written in a form comparable with Eq. (4.5) for the zero-order theory:

$$\left.\begin{array}{l} M\left[\chi_\epsilon^2/K_\epsilon\right]^2 \\ \left[K_\epsilon/\chi_\epsilon^2\right]^2 \\ \epsilon\left(0.664+1.73\,\frac{T_w}{T_o}\right)\left[\frac{K_\epsilon}{\chi_\epsilon^2}\right]^3 M^3 c_f/\sqrt{\gamma_\infty} \\ \epsilon\left(0.664+1.73\,\frac{T_w}{T_o}\right)\left[\frac{K_\epsilon}{\chi_\epsilon^2}\right]^3 M^3 c_H/\sqrt{\gamma_\infty} \end{array}\right\} = f\left[\frac{x}{L};\left(\frac{\chi_\epsilon}{K_\epsilon^{2/3}}\right),\Gamma,\frac{\chi_\epsilon^2}{K_\epsilon},\gamma,\omega,Pr\right] \quad (5.1)$$

with

$$\left.\begin{array}{l} Y_s/\tau L \\ Y_w/\tau L \\ T_w/T_o \end{array}\right\} = f\left(\frac{x}{L}\right) .$$

We see that the simplicity gained by the zero-order theory, which assumes a very strong shock and a very small ϵ, consists essentially in the elimination of the parameters γ, T_w/T_o and $\chi_\epsilon^2/K_\epsilon$. Alternative forms of Eq. (5.1) are given in Appendix II as are the similarity laws for axisymmetric flows.

There are two important limiting cases of the similitude given above. One is the case of negligible boundary-layer displacement effect, the other that of a very strong shock wave. For the first, the interaction parameter $M^{2+\omega}/\sqrt{Re_L}$ will become merely a scaling factor, and we have

$$M\delta_*/L, M^3 c_H, M^3 c_f = \frac{M^{2+\omega}}{\sqrt{Re_L}} \cdot f\left(\frac{x}{L}; M\tau, M^3 k\,\frac{t}{L}, \gamma, \omega, Pr\right)$$

A discussion of the second case follows.

Hypersonic Similitude Involving Strong Shock Waves

For this case, we require the shocks to be very strong so that terms of

$$\frac{1}{2}(\theta)^{2\frac{\gamma-1}{\gamma}} \qquad \text{and} \qquad 1/M^2\theta^2$$

may be neglected in comparison with unity. From the viewpoint of practical application, consideration of this special form is not trivial. The only essential

difference in basic requirements between this similitude and that of the zero-order theory is the condition on γ. The zero-order theory furnishes results in a convenient form for comparison with experimental data correlated by this similitude.

Under the assumption of a strong shock, the Rankine-Hugoniot shock conditions may be simplified. Using a suitable affine transformation, we arrive at a form of similitude comparable with Eqs. (4.15) and (5.1):

$$\left.\begin{array}{l} M\left[\gamma_\epsilon^2/K_\epsilon\right]^2 \quad Y_s/K_\epsilon x \\ \left[K_\epsilon/\gamma_\epsilon^2\right]^2 \quad p_w/\gamma_\infty p_\infty \\ \epsilon\left(0.664 + 1.73\,\frac{T_w}{T_0}\right)\left[\frac{K_\epsilon}{\gamma_\epsilon^2}\right]^3 \quad M^3 c_H/\sqrt{\gamma\gamma_\infty} \end{array}\right\} = f\left[\frac{x}{L};\left(\frac{\gamma_\epsilon}{K_\epsilon^{2/3}}\right)_L, \Gamma, \gamma, \omega, P_r\right] \tag{5.2}$$

with

$$\left.\begin{array}{l} Y_w/\gamma L \\ T_w/T_0 \end{array}\right\} = f\left(\frac{x}{L}\right)$$

Comparing this with the more general similitude of Eq. (5.1), we see that in the above form of similitude the dependence on the parameter $\left[\gamma_\epsilon^2/K_\epsilon\right]$, or on $k Re_t/M^{1+2\omega}$, becomes very weak as a result of the shock being very strong. On the other hand, comparison with the zero-order result, Eq. (4.15), shows that as a consequence of relaxing conditions on P_r, ω, and ϵ, we have now to include as invariants the parameters P_r, ω, ϵ, as well as T_w/T_0. The dependence on γ and on T_w/T_0 in the strong-shock similitude cannot be too strong, however, since both parameters are associated with the first-order ϵ effect.

SECTION 6

CONCLUSION

A theoretical study has been made of combined leading-edge bluntness and boundary-layer displacement effect in hypersonic flow over thin bodies. Throughout the investigation, a continuum flow of perfect gas with constant specific heats is assumed. An approach has been developed based on a flow model consisting of three adjoining regions: an inner laminar boundary layer, an outer (detached) shock layer, and between these two regions, an entropy layer. Solutions for this flow model have been obtained by considering the mutual interaction of these three regions under the requirements of the hypersonic small-disturbance theory and the shock-layer theory. In the boundary layer, a small perturbation procedure in $\epsilon = \frac{\gamma-1}{\gamma+1}$ is developed which gives the local similarity result as a leading approximation. In the entropy layer, the low density leads to the simple pressure-area relation Eq. (3.7). In the detached shock layer, the results of existing shock-layer theory are applicable. The zero-order approximation in this approach corresponds to the classical result of Busemann.

In the theory developed for the leading approximation, the problem of hypersonic plane flows over a thin body of an arbitrarily specified shape is reduced to one governed by a second-order ordinary differential equation, i.e. Eq. (4.1). The simplicity of this equation permits solutions to numerous problems of interest, including the combined effect of leading-edge bluntness, boundary-layer displacement, as well as surface inclination. Continuous transitions are exhibited between limiting solutions which agree with existing blast wave, strong viscous interaction, and hypersonic wedge theories for small ϵ . Application of this zero-order theory to the case of finite ϵ , namely $\gamma = 1.40$, shows a rather small discrepancy from the exact solutions, as far as the surface heat-

transfer rate and shock shape are concerned. One interesting feature found for inviscid flow over a blunted wedge or cone is an oscillatory pressure decay over the afterbody surface. The result can be interpreted as one limiting form of shock-layer reimpingement at glancing incidence. It may also be related to the "pressure undershoot" observed in experimental studies of hypersonic flow over blunted slender cones, and could be meaningful for studies of bluntness induced boundary-layer instability.

For the pressure and skin friction, a (consistent) first-order ϵ correction to the zero-order result appears desirable. The procedures for obtaining higher-order approximations have been formulated in Sections 2 and 3. While explicit solution to the boundary-layer equations for the higher-order correction is presently not available, simple and effective methods, such as that of Ref. 49, may be applied for this purpose. It may be pointed out that the results obtained herein are also applicable to a thin airfoil of arbitrary planform via the "strip theory". The consistency of this strip theory with the present approach has been pointed out in Ref. 41 and discussed more fully in Ref. 56.

Hypersonic similitude has been examined in Section 5 for the present problem where both bluntness and boundary-layer displacement effects are present. The classical similitude of Tsien and Hayes can be extended to include these effects for the correlation of pressure and velocity fields, as well as flow quantities of interest within the boundary layers proper, provided the vicinity of the small blunt nose is excluded. For flows involving strong shock waves, a simplified similitude is obtained. The zero-order results, which require a strong shock and also small ϵ , may be readily compared with experimental data correlated in this similitude. For consideration of experimental verification of this similitude and comparison of the experimental results with the zero-order theory, the reader may refer to Ref. 45.

REFERENCES

1. Shen, S.F., An Estimate of Viscosity Effect on Hypersonic Flow Over an Insulated Wedge. J.Math.&Phys., Vol. 31, p. 192, 1952

2. Bertram, M.H., An Approximate Method for Determining the Displacement Effects and Viscous Drag of Laminar Boundary Layers in Two-Dimensional Hypersonic Flow. NACA TN 2773, September 1952

3. Lees, L. and Probstein, R.F., Hypersonic Viscous Flow Over a Flat Plate. Aero.Eng.Lab., Princeton Rept. No. 195, 1952

4. Shen, S.F., On the Boundary-Layer Equations in Hypersonic Flow. Readers' Forum, J.Aero.Sci., Vol. 19, No. 7, p. 500, July 1952

5. Li, T.Y. and Nagamatsu, H., Shock Wave Effects on the Laminar Skin Friction of an Insulated Flat Plate at Hypersonic Speed. J.Aero.Sci., Vol. 20, p. 345, 1953

6. Lees, L., On the Boundary-Layer Equations in Hypersonic Flow and Their Approximate Solutions. J.Aero.Sci., Vol. 20, p. 143, 1953

7. Pai, S.I., A Note on Hypersonic Flow Over a Flat Plate. Readers' Forum, J.Aero.Sci., Vol. 20, No. 7, p. 502, July 1953

8. Lees, L., Hypersonic Viscous Flow Over an Inclined Wedge. J.Aero.Sci., Vol. 20, No. 11, p. 794, November 1953

9. Stewartson, K., On the Motion of a Flat Plate at High Speed in a Viscous Compressible Fluid. Pt. II. Steady Motion. J.Aero.Sci., Vol. 22, No. 5, p. 303, May 1955

10. Pai, S.I. and Shen, S.F., Hypersonic Viscous Flow Over an Inclined Wedge with Heat Transfer. 50 Jahre Grenzschichtforschung, ed. by H. Gortler and W. Tollmien, p. 112, 1955

REFERENCES (Contd)

11. Kuo, Y.H., Viscous Flow Along a Flat Plate Moving at High Supersonic Speeds. J.Aero.Sci., Vol. 23, No. 2, p. 125, February 1956

12. Pan, L.J. and Kuo, Y.H., Compressible Viscous Flow Past a Wedge Moving at Hypersonic Speeds. J.Math.&Phys., Vol. 35, p. 179, 1956

13. Lees, L., Influence of the Leading-Edge Shock Wave on the Laminar Boundary Layer at Hypersonic Speeds. J.Aero.Sci., Vol. 23, No. 6, p. 594, 1956

14. Yasuhara, M., On the Hypersonic Viscous Flow Past Slender Bodies of Revolution. J.Phys.Soc. of Japan, Vol. 11, No. 8, p. 878, August 1956

15. Lees, L., Recent Developments in Hypersonic Flow. Jet Propulsion, Vol. 27, No. 11, p. 1162, November 1957

16. Oguchi, H., First-Order Approach to a Strong Interaction Problem in Hypersonic Flow Over an Insulated Flat Plate. University of Tokyo, Aero. Res. Inst. Rept. No. 330, June 1958

17. Whalen, R.J., Boundary-Layer Interaction on a Yawed Infinite Wing in Hypersonic Flow. Readers' Forum, J.Aero/Space Sci., Vol. 26, No. 12, p. 839, December 1959

18. Lin, S.C., Cylindrical Shock Wave Produced by Instantaneous Energy Release. J.Appl.Phys., Vol. 25, No. 1, p.54, January 1954

19. Lees, L. and Kubota, T., Inviscid Hypersonic Flow Over Blunt-Nosed Slender Bodies. J.Aero.Sci., Vol. 24, No. 3, p. 195, March 1957

20. Cheng, H.K. and Pallone, A.J., Inviscid Leading-Edge Effect in Hypersonic Flow. Readers' Forum, J.Aero.Sci., Vol. 23, No. 7, p. 700, July 1956

21. Chernyi, G.G., Hypersonic Flow Past an Airfoil with a Slightly Blunted Leading Edge. Doklady, AN USSR, Vol. 114, No. 4, p. 721, 1957; English translations available as C-112, Morris D. Friedman, Inc.

22. Chernyi, G.G., Hypersonic Flow Around a Slender Blunt Cone. Doklady, AN USSR, Vol. 115, No. 4, p. 681, 1957; English translations available as C-113, Morris D. Friedman, Inc.

23. Bertram, M.H. and Baradell, D.L., A Note on the Sonic-Wedge Leading-Edge Approximation in Hypersonic Flow. Readers' Forum, J.Aero.Sci., Vol. 24, No. 8, p. 627, August 1957

24. Mirel, H. and Thornton, P.R., Effect of Body Perturbations on Hypersonic Flow Over Slender Power Law Bodies. NASA TR R-45, May 1959

25. Taylor, G.I., The Formation of a Blast Wave by a Very Intense Explosion. Pt. I. Theoretical Discussion. Proc.Roy.Soc. (A), Vol. 201, No. 1065, p. 159, March 1950

26. Sakurai, A., On the Propagation and Structure of the Blast Wave. Part I. J. Phys. Soc., Japan, Vol. 9, No. 2, p. 256, March-April 1954

27. Bertram, M.H., Viscous and Leading-Edge Thickness Effects on the Pressures on the Surface of a Flat Plate in Hypersonic Flow. J.Aero.Sci., Vol. 21, No. 6, p. 430, June 1954

28. Bogdonoff, S.M. and Hammitt, A.G., Fluid Dynamic Effect at Speeds from M = 11 to 15. J.Aero.Sci., Vol. 23, No. 2, p. 108, February 1956

29. Hammitt, A.G., Vas, I.E., and Bogdonoff, S.M., Leading-Edge Effects on the Flow Over a Flat Plate at Hypersonic Speeds. Dept. Aero. Eng., Princeton University, Rept. No. 326, 1955

30. Creager, M.O., Effects of Leading-Edge Blunting on the Local Heat Transfer and Pressure Distributions Over Flat Plates in Supersonic Flow. NACA TN 4142, December 1957

31. Henderson, A., Jr. and Johnston, Patrick J., Fluid Dynamic Properties of Some Simple Sharp- and Blunt-Nosed Shapes at Mach Numbers from 16 to 24 in Helium Flow. NASA Memo 5-8-59L, June 1959

32. Tsien, H.S., Similarity Law of Hypersonic Flow. J.Math.&Phys., Vol. 25, p. 247, 1946

33. Hayes, W.D., On Hypersonic Similitude. Quart.Appl.Math., Vol. 5, p. 105, 1947

34. Van Dyke, M.D., Application of Hypersonic Small-Disturbance Theory. J.Aero.Sci., Vol. 21, No. 3, p. 179; March 1954; Also see NACA TR 1194, NACA TN 3173 by the same author

35. Busemann, A., Flüssigleit und Gasbewegung, Handworterbuch der Naturwissenschaften Auflage, p. 275, Jena: Gustave Fischer, 1933

36. Ivey, H.R., Klunker, E.G., and Bowen, E.N., A Method for Determining the Aerodynamic Characteristics of Two- and Three-Dimensional Shapes at Hypersonic Speeds. NACA TN 1613, 1948

37. Freeman, N.C., On the Theory of Hypersonic Flow Past Plane and Axially-Symmetric Bluff Bodies. J.Fluid Mech., Vol. 1, p. 366, October 1956

38. Chester, W., Supersonic Flow Past a Bluff Body with a Detached Shock. Part I. Two-Dimensional Body. J.Fluid Mech., Vol. 1, p. 353, October 1956. Part II. Axisymmetrical Body. J.Fluid Mech., Vol. 1, p. 490, November 1956

39. Lighthill, M.J., Dynamics of a Dissociating Gas. Part I. Equilibrium Flow. J.Fluid Mech., Vol. 2, January 1957

40. Cole, J.D., Newtonian Flow Theory for Slender Bodies. J.Aero.Sci., Vol. 24, June 1957

41. Moore, F.K. and Cheng, H.K., The Hypersonic Aerodynamics of Slender and Lifting Configurations. I.A.S. Paper No. 59-125, Presented at the IAS National Summer Meeting at Los Angeles, California, 1959

42. Guiraud, J.P., 'Ecoulement Hypersonique d'un Fluide Parfait sur une Plaque Plane Comportant un Bord d'attaque d'eapisseur finie. Comptes Rendus Acad. Sci., Paris, Vol. 246, p. 2842, 1958

43. Guiraud, J.P., 'Ecoulement Hypersonique d'un Fluide Parfait sur une aile Mince Comportant un Bord d'attaque 'Emousse. Comptes Rendus, Vol. 248, p. 3524, June 1959

44. Hayes, W.D. and Probstein, R.F., Hypersonic Flow Theory: Academic, New York, 1959

45. Cheng, H.K., Hall, J.G., Golian, T.C., and Hertzberg, A., Boundary-Layer Displacement and Leading-Edge Bluntness Effects in High-Temperature Hypersonic Flow. I.A.S. Paper No. 60-38, presented at the Annual Meeting of IAS, January 1960

46. Lees, L., Laminar Heat Transfer Over Blunt-Nosed Bodies at Hypersonic Flight Speeds. Jet Propulsion, Vol. 26, No. 4, p. 259, April 1956

47. Kemp, N.H., Rose, P.H., and Detra, R.W., Laminar Heat Transfer Around Blunt Bodies in Dissociated Air. Jour. Aero/Space Sci., Vol. 26, No. 7, p. 421, July 1959

48. Vaglio-Laurin, R., Turbulent Heat Transfer on Blunt-Nosed Bodies in Two-Dimensional and General Three-Dimensional Hypersonic Flow. Jour. Aero/Space Sci., Vol. 27, No. 1, p. 27, January 1960

49. Moore, F.K., On Local Similarity in the Hypersonic Boundary Layer. Cornell Aeronautical Laboratory Report to be published

50. Chapman, D.R. and Rubesin, M.W., Temperature and Velocity Profile in Compressible Laminar Boundary Layer with Arbitrary Distribution of Surface Temperature. J.Aero.Sci., Vol. 16, p. 547, 1949

51. Eckert, E.R.G., Engineering Relations for Friction and Heat Transfer to Surface in High Velocity Flow. J.Aero.Sci., Vol. 22, pp. 585-587, 1955

52. Howarth, L., Modern Developments in Fluid Dynamics. High-Speed Flow, Vol. 1, p. 422, Oxford University Press, London, 1953

53. Bertram, M.H., Tip-Bluntness Effects on Cone Pressure at M = 6.85. J.Aero.Sci., Readers' Forum, Vol. 23, No. 9, p. 898, September 1956

54. Cheng, H.K., Similitude of Hypersonic Real-Gas Flows Over Slender Bodies with Blunted Noses. J.Aero/Space Sci., Vol. 26, No. 9, p. 575, September 1959

55. Hayes, W.D. and Probstein, R.F., Viscous Hypersonic Similitude. J.Aero/Space Sci., Vol. 26, No. 12, p. 815, December 1959

56. Cheng, H. K., The Shock-Layer Concept and Three-Dimensional Hypersonic Boundary Layers. Cornell Aeronautical Laboratory Report No. AF-1285-A-3 (to be published)

APPENDIX I

ON THE COMPLETE SOLUTION TO $Y(YY')' = \epsilon k t/2$

Throughout the study presented in the text, it is tacitly assumed that the solution to

$$(Y_e - Y_b)^{\gamma} \cdot p_e = \text{constant} \tag{I.1}$$

behaves like $Y_e \sim x^{2/3}$, as required by the existing blast-wave theory[1-3]. This implies, for the special case $\gamma \to 1$ and $Y_b = 0$, that the only solution of

$$Y_e (Y_e Y_e')' = \epsilon k t/2 \tag{I.2}$$

admissible to the present study is that of Eq. (4.5) of the text, i.e.

$$Y_e = \left(\frac{3}{2}\right)^{2/3} (\epsilon k t)^{1/3} x^{2/3} . \tag{I.3}$$

On the other hand, a complete solution can actually be obtained for Eq. (I.2), which not only includes the blast-wave result Eq. (I.3), but also exhibits the feature of a "free layer" in the limit of $x \to 0$. It thus appears that by employing the complete solution, it would be possible to describe, in analytic terms, the transition from Lighthill's free layer[39] in the neighborhood of a blunt nose to the blast-wave dominated region far downstream. However, as far as application to the present problem is concerned, it is also essential to examine the compatibility of this solution with the small-perturbation requirement (A) which underlies Eqs. (I.1) and (I.2). The main conclusion of the following discussion is that, unless the small-perturbation requirement is removed, or relaxed,

the improvement gained by using the complete solution cannot be established, and the particular solution pertaining to the existing blast-wave theory appears to be the only valid result under requirement (A)-(C). Below, the complete solution to Eq. (I.2) will be presented first, and the question of consistency with the small-perturbation requirement will then be examined. The existence of an explicit integral form of Eq. (I.2) for the complete solution was pointed out to the writer recently by Mr. J. P. Guiraud of ONERA, France.

For convenience, we shall drop the subscript e from Y_e. Since the differential equation, Eq. (I.2), does not contain the independent variable x, we may let $p = YY'$, and the equation can be integrated to yield

$$p^2 = \epsilon k t (Y + C_1)$$

that is,

$$YY' = \sqrt{\epsilon k t (Y + C_1)} \tag{I.4}$$

Integrating once, after separation of the variable, one has the complete solution

$$(Y+C_1)^{3/2} - 3C_1(Y+C_1)^{1/2} = \frac{3}{2}\sqrt{\epsilon k t}\ (x + C_2) \tag{I.5}$$

For large x, $Y \gg C_1$, Eq. (I.5) provides the blast-wave result, i.e., Eq. (I.3). Now, for sufficiently small x, Eq. (I.5) may be developed for $Y \ll C_1$, namely

$$C_1^{3/2}\left[1 + \frac{3}{2}\left(\frac{Y}{C_1}\right) + \frac{3}{2}\left(\frac{3}{2}-1\right)\frac{1}{2!}\left(\frac{Y}{C_1}\right)^2 + \cdots\right]$$
$$- 3C_1^{3/2}\left[1 + \frac{1}{2}\left(\frac{Y}{C_1}\right) + \frac{1}{2}\left(\frac{1}{2}-1\right)\frac{1}{2!}\left(\frac{Y}{C_1}\right)^2 + \cdots\right]$$
$$= \frac{3}{2}\sqrt{\epsilon k t}\ (x + C_2).$$

We see that the constants C_1 and C_2 have to be related as

$$C_2 = -\frac{4}{3} C_1^{3/2} \Big/ \sqrt{\epsilon k t}$$

and, what seems to be more significant, that, for small x ,

$$Y = (\epsilon k t\, C_1)^{1/4} x^{1/2} + \cdots .$$

This is no more or less than the equation of a free layer. Now, if the domain of validity for the solution in the blunt-nose region and that for the hypersonic small-distance theory should join, the above asymptotic solution for small x must be identified as Lighthill's free layer in the vicinity of the leading edge. Accordingly, C_1 belongs to the order $(t/\epsilon k)$, so that the equation for the free layer may be written as

$$\left.\begin{aligned} Y &= a^{1/4} t^{1/2} x^{1/2} + \cdots . \\ a &= O(1) \end{aligned}\right\} \qquad \text{(I.6)}$$

The above relation implies that the shock layer detaches from the body at $x = O(t)$ with $dy/dx = O(1)$. The complete solution may now be expressed as

$$\left[Y + (at/\epsilon k)\right]^{3/2} - 3(at/\epsilon k)\left[Y + (at/\epsilon k)\right]^{1/2} = \frac{3}{2}\sqrt{\epsilon k t}\left[x - \frac{4}{3} a^{3/2} t/\epsilon^2 k^2\right] \qquad \text{(I.7)}$$

The blast-wave result, Eq. (I.3), would be obtained from Eq. (I.7) by neglecting terms of the order $(at/\epsilon k Y)$.

The question of whether, and when, the more complete solution Eq. (I.7) is compatible with the small-perturbation requirement (A) will be examined. In this respect, the asymptotic solution for large $(\epsilon k Y/at)$, i.e., the blast-wave

result, has been studied in Section 2 of the text, where the range of its validity has been established. We shall, therefore, be concerned with two remaining questions: (1) can requirement (A) be satisfied, when the difference between Eqs. (I.7) and (I.3) is not small, and (2) when the blast-wave solution dominates, does the contribution from the $at/\epsilon k Y$ terms belong to an order lower than that of the error in the hypersonic small-disturbance theory.

The first question amounts to

$$\left.\begin{aligned} &\text{if} \quad \epsilon k Y/at \leq O(1) \,, \\ &\frac{1}{2}\left(\frac{dY}{dx}\right)^{2\frac{\gamma-1}{\gamma}} \ll 1 \ ? \end{aligned}\right\} \tag{I.8}$$

Since $\epsilon k Y/at \leq O(1)$, $Y = O\left[t^{1/2} x^{1/2}\right]$, and

$$\left(\frac{dY}{dx}\right) = O\left(\frac{t}{Y}\right) = \frac{at}{\epsilon k Y}\, O(\epsilon k) \geq O(\epsilon k) \tag{I.9}$$

Hence,

$$\left(\frac{dY}{dx}\right)^{2\frac{\gamma-1}{\gamma}} \geq O(\epsilon k)^{2\frac{\gamma-1}{\gamma}} = O(1) \,. \tag{I.10}$$

Therefore, when the free-layer character begins to predominate the solution for flat-plate afterbodies, the small-disturbance requirement cannot be satisfied.

The second question concerns

$$\begin{aligned} &\text{if} \quad \epsilon k Y/at \gg 1 \\ &\frac{1}{2}\left(\frac{dY}{dx}\right)^{2\frac{\gamma-1}{\gamma}} \ll \left(\frac{at}{\epsilon k Y}\right) \ ? \end{aligned} \tag{I.11}$$

Since $\epsilon k Y/at \gg 1$, $Y \sim (\epsilon k t)^{1/3} x^{2/3}$, and

$$\left(\frac{dY}{dx}\right) \sim \left(\frac{\epsilon k t}{Y}\right)^{1/2} = \left(\frac{at}{\epsilon k Y}\right)^{1/2} \frac{\epsilon k}{\sqrt{a}} \tag{I.12}$$

thus

$$\left(\frac{dY}{dx}\right)^{2\frac{\gamma-1}{\gamma}} \sim \left(\frac{at}{\epsilon k Y}\right)^{\frac{\gamma-1}{\gamma}} \left(\frac{\epsilon k}{\sqrt{a}}\right)^{2\frac{\gamma-1}{\gamma}} = O\left[\left(\frac{at}{\epsilon k Y}\right)^{\frac{\gamma-1}{\gamma}}\right] \gg \left(\frac{at}{\epsilon k Y}\right) \qquad \text{(I.13)}$$

Therefore, the $(at/\epsilon k Y)$ terms in the blast-wave dominated range are too small to be considered as a valid improvement of the small-disturbance theory.

Our conclusions are: (1) The complete solution, Eqs. (I.5) or (I.7), exhibits an apparently realistic behavior of the detached shock layer over a flat-plate afterbody, providing a transition from the Lighthill's free layer to the blast-wave solution; (2) Unless the small-perturbation requirement (A) is removed, or relaxed, the complete solution cannot, however, represent an improvement over the existing blast-wave result; (3) The solution may, perhaps, find a valid application to the corresponding problem in the "piston theory" where the small-disturbance assumption is not required.

APPENDIX II

ALTERNATIVE FORMS OF HYPERSONIC SIMILITUDE FOR CORRELATING SHOCK SHAPE, DISPLACEMENT THICKNESS, SKIN FRICTION, SURFACE PRESSURE AND HEAT-TRANSFER RATE IN PLANE AND AXISYMMETRIC FLOWS

On the basis of the hypersonic small-disturbance theory and the boundary-layer theory for ideal gases with constant specific heats, constant Prandtl's number and the viscosity-temperature relation $\mu \propto T^{\omega}$, similarity can exist among flow fields around thin or slender bodies. For bodies having similar shapes and similar surface temperature distributions, i.e.

$$\left.\begin{matrix} Y_w/\tau L \\ T_w/T_0 \end{matrix}\right\} = g\left(\frac{x}{L}\right) \tag{II.1}$$

one may thus correlate the corresponding shock shapes, surface pressure and heat-transfer rate as

$$\left.\begin{matrix} M Y_s/L \\ p_w/p_\infty \\ M^3 c_H \end{matrix}\right\} = f\left(\frac{x}{L}\,;\, M\tau\,,\, \frac{M^{2+\omega}}{\sqrt{Re_L}}\,,\, M^{\frac{3+\nu}{1+\nu}} k^{\frac{1}{1+\nu}} \frac{t}{L}\,,\, \gamma\,,\, \omega\,,\, Pr\right) \tag{II.2}$$

where g and f represents arbitrary functions of the variables involved, different for different flow quantities. The displacement thickness of the boundary layer δ_* and the skin-friction coefficient c_f can be correlated in the same forms as for the shock shape Y_s and the coefficient of surface heat-transfer c_H, respectively, and therefore will not be repeated hereafter.

It may be useful, for application in experimental studies, to consider certain alternative forms of the similitude cited. A few of these forms, with Eq. (II.1) unchanged, are given below:

$$\left.\begin{matrix} p_w/p_\infty M^2\tau^2 \\ Y/\tau L \\ c_H/\tau^3 \end{matrix}\right\} = f\left(\frac{x}{L};\ \frac{M^\omega}{\tau^2\sqrt{Re_L}},\ \frac{k^{\frac{1}{1+\nu}}\frac{t}{L}}{\tau^{\frac{3+\nu}{1+\nu}}},\ M\tau;\ \gamma,\omega,Pr\right) \qquad \text{(II.2a)}$$

$$\left.\begin{matrix} p_w/p_\infty M^2\tau^2 \\ (\tau)^{\frac{2\nu}{1+\nu}} Y_s/(\epsilon k)^{\frac{1}{1+\nu}} t \\ \Pi^{\frac{1}{2}} \frac{M^3 c_H}{(M\tau)^{\frac{5+3\nu}{2+2\nu}}} \end{matrix}\right\} = f\left(\frac{x}{L};\ [M\tau]^{\frac{3+\nu}{1+\nu}}/K_{\epsilon_L},\ \Gamma,\Pi,\epsilon,\omega,Pr\right) \qquad \text{(II.2b)}$$

$$\left.\begin{matrix} p_w/p_\infty M^2\tau^2 \\ M^4\tau^3 Y_s/\chi_\epsilon^2 L \\ c_H/\tau^3 \end{matrix}\right\} = f\left(\frac{x}{L};\ \frac{\chi_\epsilon}{M^2\tau^2},\ \Gamma,\Pi,\epsilon,\omega,Pr\right) \qquad \text{(II.2c)}$$

$$\left.\begin{matrix} \Pi^{\frac{2+2\nu}{1+3\nu}} p/p_\infty \\ M Y_s/\Pi^{\frac{3+3\nu}{1+3\nu}} \chi_\epsilon^2 L \\ \Pi^{\frac{3+3\nu}{1+3\nu}} M^3 c_H \end{matrix}\right\} = f\left(\frac{x}{L};\ \chi_{\epsilon_L}/K_{\epsilon_L}^{\frac{2+2\nu}{3+\nu}},\ \Gamma,\Pi,\epsilon,\omega,Pr\right) \qquad \text{(II.2d)}$$

where χ_{ϵ_L} is the same as χ_ϵ defined in Section 4, with $\ell = L$, and

$$\left.\begin{aligned} K_{\epsilon_L} &\equiv M^{\frac{3+\nu}{1+\nu}} (\epsilon k)^{\frac{1}{1+\nu}} \frac{t}{L} \\ \Pi &\equiv K_{\epsilon_L} \Big/ \chi_{\epsilon_L}^2 \\ \Gamma &\equiv \frac{1}{2} \Pi (M\tau)^{\frac{1+3\nu}{1+\nu}} \end{aligned}\right\}$$

The forms of Eqs. (II.2a) - (II.2d) given above have the property that, for cases involving very strong shock waves, $M\tau$ or Π will drop out from the right of Eqs. (II.2a) - (II.2d), and the total number of the similarity parameters can therefore be reduced by one. The forms (II.2b) - (II.2d) have the additional advantage that, for strong shocks, small ϵ, unit Prandtl number, linear representation of the viscosity-temperature relation, and uniform T_w/T_o, not only the constants Pr and ω drop out from the similitude but also the parameters ϵ and T_w/T_o are not required to remain fixed in the simulation. The last three forms correspond to the forms of particular solutions presented in Figs. 3-6.

TABLE I

COMPARISON OF SKIN FRICTIONS AND SURFACE HEAT-TRANSFER RATES OF A FLAT PLATE AT HIGH MACH NUMBER PREDICTED BY SOLUTIONS ASSUMING LINEAR VISCOSITY-TEMPERATURE RELATIONS AND THOSE BASED ON YOUNG'S FORMULA FOR $\mu \propto T^{\omega}$

Table I(a) Asymptotic Formulas for high M

	Chapman & Rubesin[42]	Present	Young[44]
Reference Temperature	T_w	$\frac{T_o}{6}\left[1 + 3\,\frac{T_w}{T_o}\right]$	
$c_f\sqrt{Re}\,/\,0.664\left[\frac{\gamma-1}{2}M_1^2\right]^{\frac{\omega-1}{2}}$	$\left(\frac{T_w}{T_o}\right)^{\frac{\omega-1}{2}}$	$\left[\frac{1}{6} + \frac{1}{2}\,\frac{T_w}{T_o}\right]^{\frac{\omega-1}{2}}$	$(P_r)^{\frac{\omega-1}{4}}\left[0.18 + \frac{0.55}{\sqrt{P_r}}\,\frac{T_w}{T_o}\right]^{\frac{\omega-1}{2}}$
$2\,c_H/c_f$	1	1	$\left[1-\frac{T_w}{\sqrt{P_r}\,T_o}\right]\Big/(P_r)^{1/6}\left[1-\frac{T_w}{T_o}\right]$

Table I(b) Comparison of the skin friction predictions for $P_r = 0.71$ and $\omega = 0.76$, at high M

$\frac{T_w}{T_o}$	(c_f) Chapman & Rubesin	(c_f) Present	(c_f) Young
0	∞	1.03	1
1/10	1.14	1.06	1
1/6	1.10	1.05	1
1	0.99	1.05	1

TABLE II

COMPARISON OF THE ZERO-ORDER SOLUTIONS WITH THE SELF-SIMILAR SOLUTIONS TO THE PROBLEM OF STRONG SHOCK-BOUNDARY LAYER INTERACTION OVER A FLAT PLATE FOR $\gamma = 1.40$ AT DIFFERENT WALL-TO-STAGNATION TEMPERATURE RATIOS

$\frac{T_w}{T_o}$	$\frac{MY_s}{x\,\bar{\chi}^{1/2}}$	$\frac{p_w}{p_\infty\,\bar{\chi}}$	$\frac{M_\infty^3\,c_H}{\bar{\chi}^{3/2}}$	$\frac{M_\infty^3\,c_f}{\bar{\chi}^{3/2}}$	Sources From Which Data are Given or Deduced	$\frac{Y_s^{(0)}}{Y_s}$	$\frac{p_w^{(0)}}{p_w}$	$\frac{c_H^{(0)}}{c_H}$	$\frac{c_f^{(0)}}{c_f}$
0	0.62	0.158	0.0965	0.216	Whalen[26]	0.82	0.85	0.89	0.80
		(0.183)	(0.10)	(0.20)	Lees[15]				
0.20	- -	0.232	0.118	0.283	Whalen[26]	- -	0.88	0.90	0.75
0.40	- -	0.312	- - -	- - -	Whalen[26]	- -	0.88	- -	- -
1.00	- -	0.546	- - -	0.855	Stewartson[18]	- -	0.89	- -	0.38

NOTE: 1. Lees' theory based on tangent-wedge formula for pressure.

2. $p^{(0)}$, $c_H^{(0)}$, etc. represent zero-order solutions given in text.

3. Zero-order theory differs from others only in assumption γ close to one (all theories assume $Pr = 1$, $\mu \propto T$).

TABLE III

COMPARISON OF THE ZERO-ORDER SOLUTIONS WITH THE SELF-SIMILAR SOLUTIONS TO THE FLAT-PLATE AFTERBODY PROBLEM FOR $\gamma = 1.40$

$\frac{T_w}{T_0}$	$\frac{Y_s}{k^{1/3}\left(\frac{\nu}{t}\right)^{2/3} t}$	$\frac{p_w}{p_\infty K^{2/3}}$	$\frac{M_\infty^3 c_H}{\bar{\zeta} K^{1/3}}$	$\frac{c_f}{c_H}$	Sources From Which Data are Given or Deduced	$\frac{Y_s^{(0)}}{Y_s}$	$\frac{p_w^{(0)}}{p_w}$	$\frac{c_H^{(0)}}{c_H}$	$\frac{c_f^{(0)}}{c_f}$
0	0.73	0.112	.0671	2.39	Cheng & Pallone[3]	1.05	1.44	1.15	0.97
	(0.775)	(0.121)	(0.0697)	(2.39)	(Sakurai[46])	(0.99)	(1.33)	(1.10)	(0.93)
0.15	0.73	0.112	.0682	2.56	Cheng & Pallone[3]	1.05	1.44	1.14	0.89
0.40	"	"	.0704	2.87	" " "	"	"	1.10	0.77
1.0	"	"	.0748	3.60	" " "	"	"	1.04	0.58

NOTE:

1. c_H and c_f are obtained from the self-similar solutions to the boundary-layer problem under the pressure given.

2. $K \equiv M_\infty^3 k \frac{t}{x} = K_\epsilon / \epsilon$ (for $\nu = 0$).

3. The numerical coefficient in the shock-shape result for $\gamma = 1.40$ given by Cheng & Pallone is in error; the corrected formula is
$$Y_s = 0.73 k^{1/3} (x/t)^{2/3} t .$$

4. $p^{(0)}$, $c_H^{(0)}$, etc. represent zero-order solutions given in Eq. (4.5).

5. If data deduced from Sakurai's blast-wave solution are used as a basis for comparison, the zero-order approximation will generally appear better.

6. For the case of cylindrical afterbodies, the blast-wave solution of Sakurai gives
$$Y_s = 0.795 k^{1/2} (x/t)^{1/2} t \quad p_w = 0.0689 p_\infty M^2 k^{1/2} \frac{d}{x} \text{ , and}$$
$$Y_s^{(0)} / Y_s = 0.958, \quad p_w^{(0)} / p_w = 1.46.$$

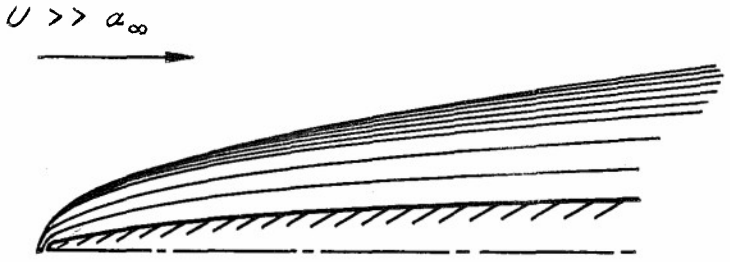

(a)

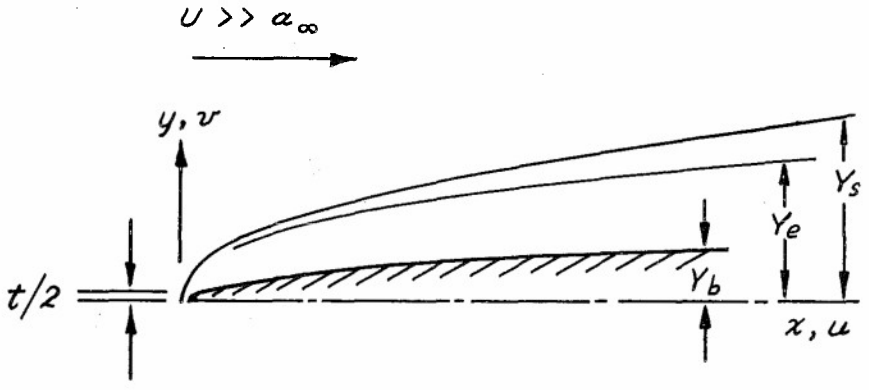

ENTROPY LAYER: $Y_b < y < Y_e$

SHOCK LAYER: $Y_e < y < Y_s$

(b)

Figure 1 (a) ILLUSTRATIONS OF THE STREAM-LINE PATTERN OF THE FLOW FIELD AROUND A SLENDER BODY WITH SMALL BLUNT NOSE
(b) DIVISION OF THE INVISCID-FLOW REGION ABOUT A SLENDER AFTERBODY INTO A SHOCK LAYER AND AN ENTROPY LAYER

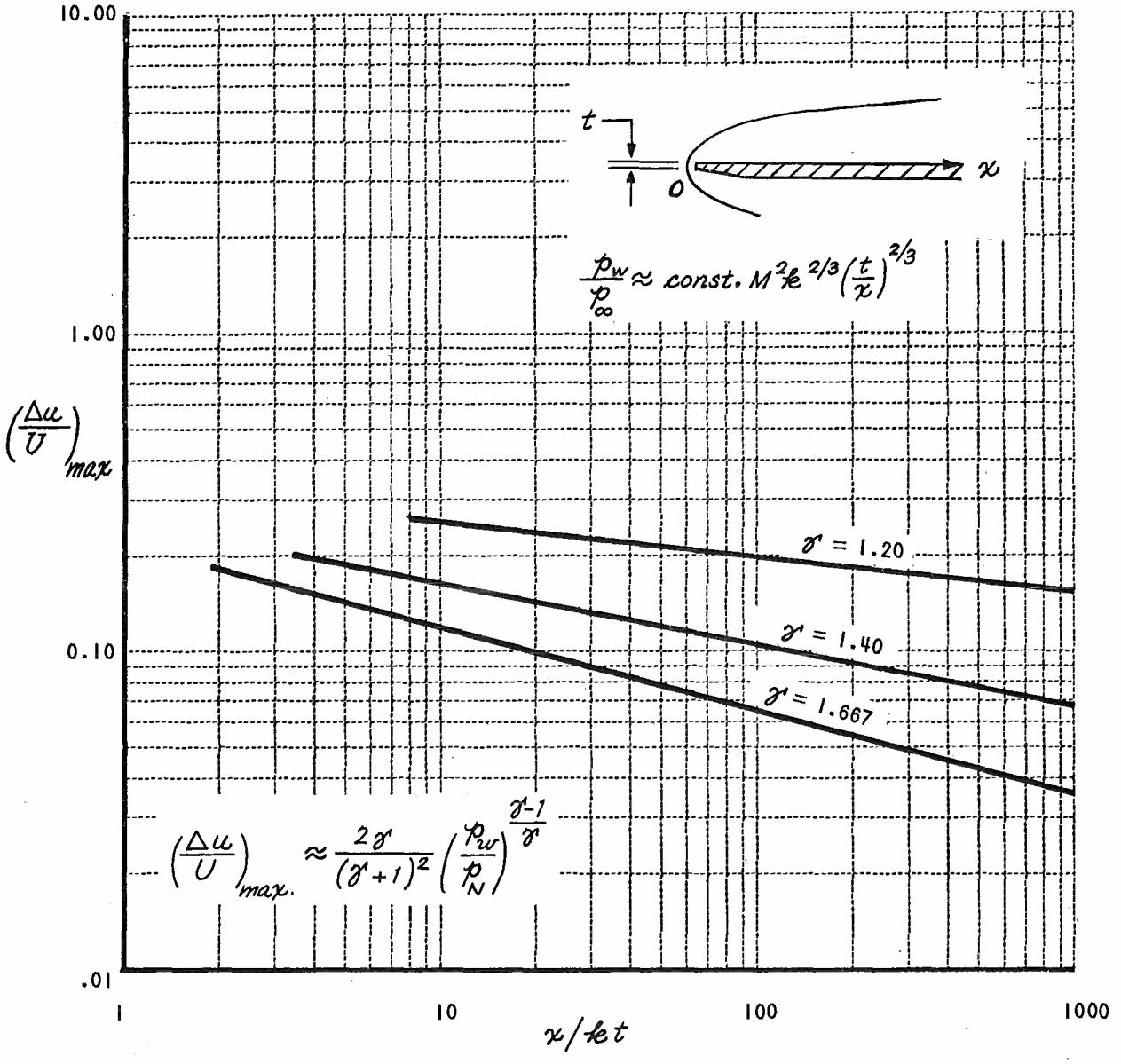

FIGURE 2 DETERMINATION OF THE MAXIMUM PERTURBATION VELOCITY $|\Delta u| \equiv U_\infty - u$ OVER A FLAT-PLATE AFTERBODY IN AN INVISCID HYPERSONIC FLOW

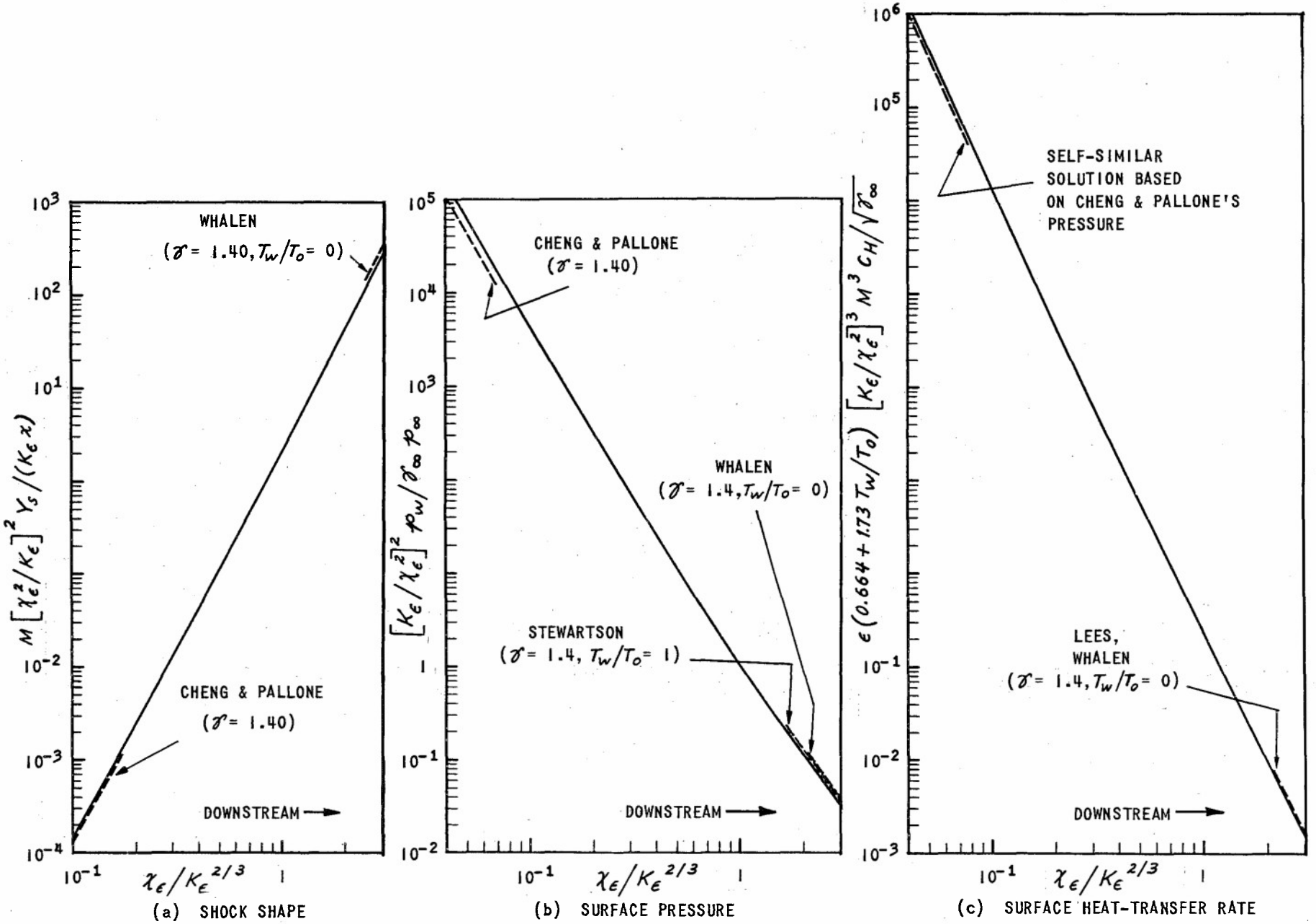

Figure 3 RESULTS BASED ON THE ZERO-ORDER THEORY OF A FLAT PLATE UNDER THE COMBINED EFFECT OF TIP BLUNTNESS AND BOUNDARY-LAYER DISPLACEMENT (REFER TEXT FOR BASIC ASSUMPTIONS, RESTRICTIONS AND NOTATIONS)

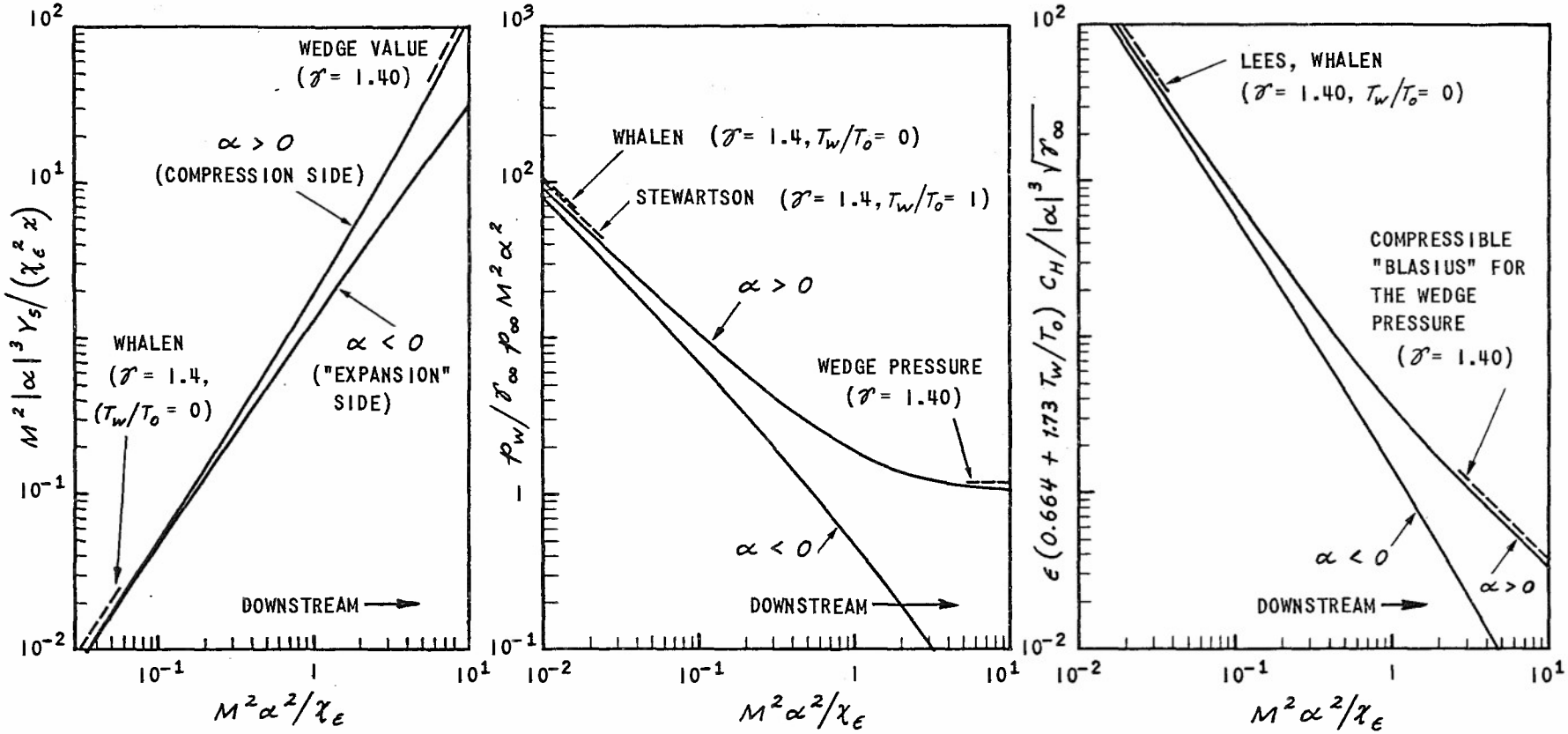

(a) SHOCK SHAPE (b) SURFACE PRESSURE (c) SURFACE HEAT-TRANSFER RATE

Figure 4 RESULTS BASED ON THE ZERO-ORDER THEORY OF A FLAT PLATE AT INCIDENCE UNDER THE COMBINED EFFECT OF BOUNDARY-LAYER DISPLACEMENT AND ANGLE OF ATTACK

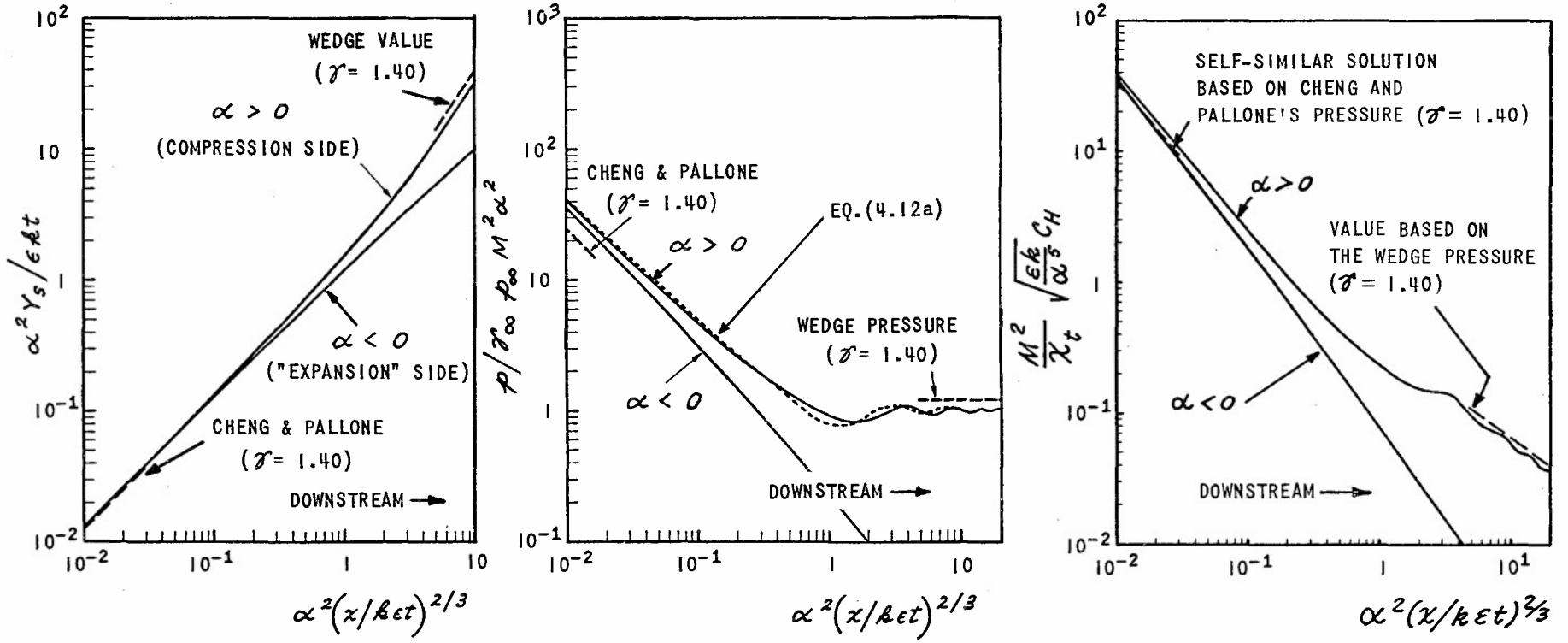

(a) SHOCK SHAPE (b) SURFACE PRESSURE (c) SURFACE LAMINAR HEAT-TRANSFER RATE

Figure 5 RESULTS BASED ON THE ZERO-ORDER THEORY OF A FLAT PLATE UNDER THE COMBINED EFFECT OF LEADING-EDGE BLUNTNESS AND ANGLE OF ATTACK

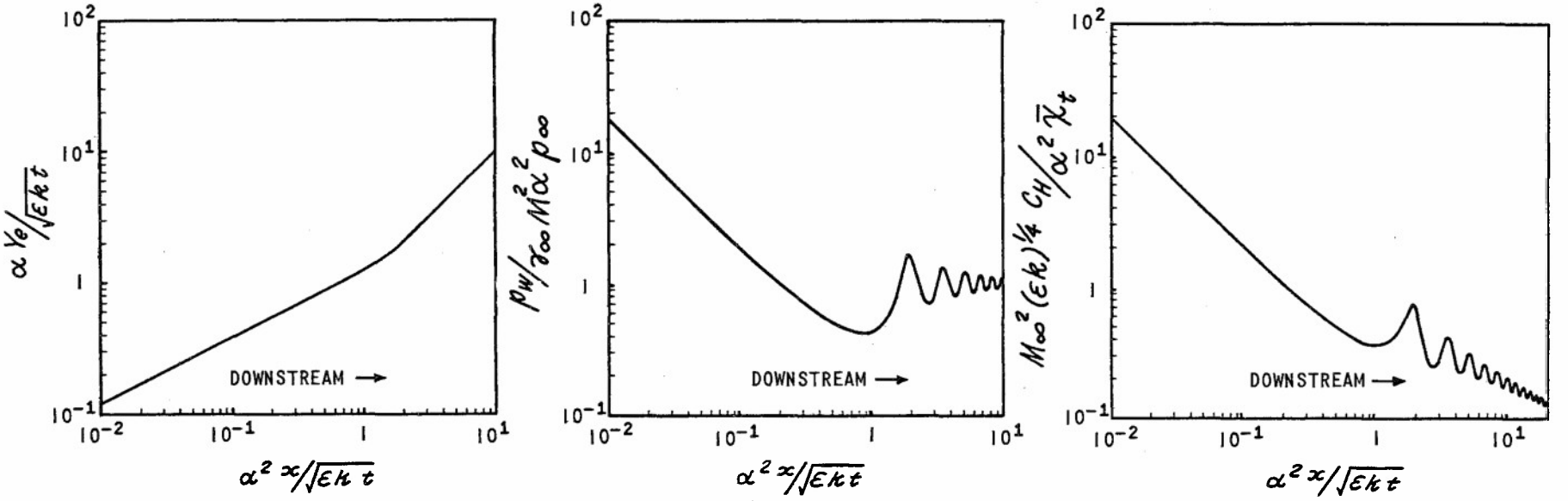

(a) SHOCK SHAPE

(B) SURFACE PRESSURE

(C) SURFACE LAMINAR HEAT-TRANSFER RATE

Figure 6 RESULTS BASED ON THE ZERO-ORDER THEORY OF A BLUNTED SLENDER CONE

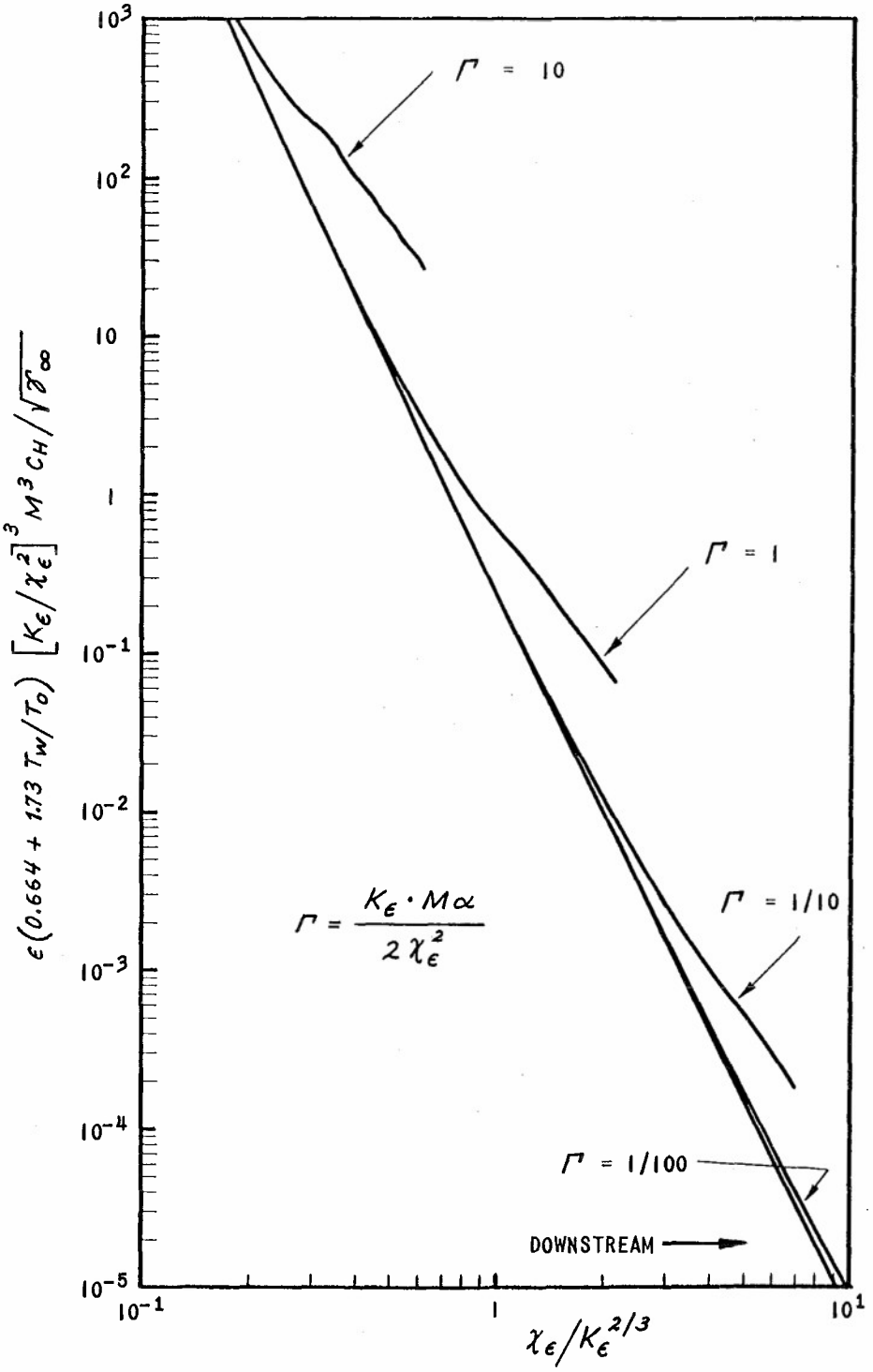

(a) SURFACE HEAT-TRANSFER RATE

Figure 7 RESULTS BASED ON THE ZERO-ORDER THEORY OF HYPERSONIC FLOW OVER THIN WEDGE SUBJECT TO LEADING-EDGE BLUNTNESS AND BOUNDARY-LAYER DISPLACEMENT EFFECTS.

DISTRIBUTION LIST

NAVY

Chief of Naval Research
Department of the Navy
Washington 25, D. C.
Attn: Code 438 (2)
Code 419 (1)
Code 461 (1)

Commanding Officer
Office of Naval Research
Branch Office
150 Causeway Street
Boston, Massachusetts (1)

Commanding Officer
Office of Naval Research
Branch Office
The John Crerar Library Building
86 East Randolph Street
Chicago 1, Illinois (1)

Commanding Officer
Office of Naval Research
Branch Office
346 Broadway
New York 13, N. Y. (1)

Commanding Officer
Office of Naval Research
Branch Office
1030 East Green Street
Pasadena 1, California (1)

Commanding Officer
Office of Naval Research
Branch Office
1000 Geary Street
San Francisco 9, California (1)

Commanding Officer
Office of Naval Research
Navy No. 100, Box 39
Fleet Post Office
New York, New York (15)

Director
Naval Research Laboratory
Washington 25, D. C.
Attn: Code 2021 (6)

Chief, Bureau of Aeronautics
Department of the Navy
Washington 25, D. C.
Attn: Research Division
Aero. & Hydro. Branch (1)

Commanding Officer and Director
David Taylor Model Basin
Caderock, Maryland
Attn: Aerodynamics Laboratory (1)

Chief, Bureau of Naval Weapons
Department of the Navy
Washington 25, D. C.
Attn: Code Re 0 (1)
Code Re Sl-e (1)

Commander
U. S. Naval Weapons Laboratory
Dahlgren, Virginia
Attn: Technical Library (1)

Commander
Naval Ordnance Test Station
Inyokern, China Lake, California
Attn: Technical Library (1)
Code 501 (1)

Commander
Naval Ordnance Laboratory
White Oak, Maryland
Attn: Hyperballistics Division (1)
Aeroballistics Division (1)
Aerophysics Division (1)

Chief, Bureau of Yards and Docks
Department of the Navy
Washington 25, D. C.
Attn: Plans and Research (1)

NAVY (cont)

Superintendent
Naval Postgraduate School
Monterey, California (1)

U. S. Naval Air Material
Test Center
Point Mugu, California
Attn: Chief Scientist (1)

AIR FORCE

Director, Office for Advanced
Studies
Air Force Office of Scientific
Research
Box 2035
Pasadena 2, California (1)

Commander
Western Development Division (ARDC)
P. O. Box 262
Inglewood, California (1)

Commander
Air Force Cambridge Research Center
230 Albany Street
Cambridge 39, Massachusetts
Attn: Geophysical Res. Library (1)

NASA

Director
Langley Research Center
National Aeronautics and Space
Administration
Langley Field, Virginia (1)

Director
Ames Research Center
National Aeronautics and Space
Administration
Moffett Field, California (1)

Director
Lewis Research Center
National Aeronautics and Space
Administration
Cleveland Airport
Cleveland 11, Ohio (1)

Western Coordination Office
National Aeronautics and Space
Administration
7660 Beverly Blvd.
Los Angeles 36, California (1)

DEPT. OF DEFENSE

Chief
Armed Forces Special Weapons
Project
P. O. Box 2610
Washington 25, D. C. (1)

Executive Secretary
Weapons System Evaluation Group
Office of the Secretary of Defense
The Pentagon
Washington 25, D. C. (1)

OTHER GOV'T AGENCIES

Director
National Bureau of Standards
Washington 25, D. C.
Attn: Fluid Mechanics Section (1)
Electron Physics Section (1)

National Science Foundation
Division of Mathematical, Physical
and Engineering Sciences
Washington 25, D. C. (1)

Documents Service Center
Armed Services Technical
Information Agency
Arlington Hall Station
Arlington 12, Virginia (10)

EDUCATIONAL INSTITUTIONS

Division of Engineering
Brown University
Providence 12, Rhode Island
Attn: Profs. Maeder, Kestin, Probstein (1)

Metcalf Laboratory
Brown University
Providence 12, Rhode Island
Attn: Prof. D. F. Hornig (1)

Low Pressure Research Project
University of California
Engineering Field Station
1301 South 46th Street
Richmond, California (1)

Radiation Laboratory
University of California
Livermore, California
Attn: Drs. S. A. Colgate, R. Post (1)

Los Alamos Scientific Laboratory
University of California
Los Alamos, New Mexico
Attn: Theoretical Div.
(Dr. J. L. Tuck) (1)
Dr. R. G. Shreffler (1)
J-1 Division (Drs. Duff, Graves) (1)

Guggenheim Aeronautical Laboratory
California Institute of Technology
Pasadena 4, California
Attn: Prof. C. B. Millikan, Dir. (1)
Prof. L. Lees (1)

Department of Physics
California Institute of Technology
Pasadena 4, California
Attn: Prof. F. Zwicky (1)

Department of Aerodynamics
Case Institute of Technology
Cleveland 6, Ohio
Attn: Prof. G. Kuerti (1)

Yerkes Observatory
University of Chicago
Williams Bay, Wisconsin
Attn: Prof. S. Chandrasekhar (1)

Cornell University
Ithaca, New York
Attn: Engineering Library (1)

Department of Engineering Sciences
Harvard University
Cambridge 38, Massachusetts
Attn: Prof. G. Carrier (1)
Prof. H. Emmons (1)

Harvard Observatory
Harvard University
Cambridge, Massachusetts
Attn: Prof. F. Whipple (1)

Department of Aeronautical Engineering
University of Illinois
Urbana, Illinois
Attn: Prof. H. S. Stillwell, Chairman (1)

Applied Physics Laboratory
Johns Hopkins University
P. O. Box 244, Rt. 1
Laurel, Maryland
Attn: Dr. F. N. Frenkiel (1)
Tech. Reports Office (1)

Institute for Fluid Mechanics and Applied Mathematics
University of Maryland
College Park, Maryland
Attn: Profs. Burgers, Pai (1)

Department of Mathematics
Massachusetts Institute of Technology
Cambridge 39, Massachusetts
Attn: Prof. C. C. Lin (1)

EDUCATIONAL INSTITUTIONS (cont)

Department of Aeronautical Engineering
Massachusetts Institute of Technology
Cambridge 39, Massachusetts
Attn: Prof. H. G. Stever (1)

Department of Mechanical Engineering
Massachusetts Institute of Technology
Cambridge 39, Massachusetts
Attn: Prof. J. Kaye (1)

Department of Aeronautical Engineering
University of Michigan
Ann Arbor, Michigan
Attn: Prof. W. C. Nelson (1)

Therm Advanced Research
Therm, Incorporated
Ithaca, New York
Attn: Dr. A. Ritter (1)

Engineering Research Institute
University of Michigan
Ann Arbor, Michigan
Attn: Prof. O. Laporte (1)
Prof. G. Uhlenbeck (1)

Department of Astronomy
University of Michigan
Ann Arbor, Michigan
Attn: Prof. L. Goldberg (1)

Department of Aeronautical Engineering
University of Minnesota
Minneapolis, Minnesota
Attn: Prof. J. D. Akerman, Chairman (1)

Institute of Meteorites
University of New Mexico
Albuquerque, New Mexico
Attn: Prof. L. LaPaz (1)

Institute for Mathematics and Mechanics
New York University
25 Waverly Place
New York 3, New York
Attn: Prof. R. Courant, Dir. (1)

Guggenheim School of Aeronautics
New York University
New York 53, New York
Attn: Prof. J. F. Ludloff (1)

Department of Mechanical Engineering
Northwestern University
Evanston, Illinois
Attn: Prof. A. B. Cambel (1)

Department of Physics
University of Oklahoma
Norman, Oklahoma
Attn: Prof. R. G. Fowler (1)

Aerodynamics Laboratory
Polytechnic Institute of Brooklyn
Freeport, L.I., New York
Attn: Prof. A. Ferri (1)

Palmer Physics Laboratory
Princeton University
Princeton, New Jersey
Attn: Prof. W. Bleakney (1)
Prof. W. C. Griffith (1)

Department of Aeronautical Engineering
Princeton University
Princeton, New Jersey
Attn: Profs. S. Bogdonoff, W. Hayes (1)

Princeton University Observatory
Princeton, New Jersey
Attn: Prof. L. Spitzer, Jr. (1)

Department of Aeronautical Engineering
Rensselaer Polytechnic Institute
Troy, New York
Attn: Prof. R. P. Harrington (1)

EDUCATIONAL INSTITUTIONS (cont)

Engineering Center
University of Southern California
University Park
Los Angeles 7, California
Attn: Dr. R. Chaun (1)

Guggenheim Aeronautical Laboratory
Stanford University
Stanford, California (1)

Defense Research Laboratory
University of Texas
P. O. Box 8029
Austin, Texas
Attn: M. J. Thompson (1)

College of Engineering
U.C.L.A.
Los Angeles, California
Attn: Dean L. M. K. Boelter (1)

Department of Physics
U.C.L.A.
Los Angeles, California
Attn: Prof. J. Kaplan (1)

Experimental Research Group
University of Utah
Salt Lake City, Utah
Attn: Prof. M. A. Cook, Dir. (1)

Department of Chemistry
University of Wisconsin
Madison, Wisconsin
Attn: Prof. J. O. Hirschfelder (1)

Sterling Chemistry Laboratory
Yale University
New Haven, Connecticut
Attn: Prof. J. G. Kirkwood (1)

INDUSTRIAL ORGANIZATIONS

Aerojet Engineering Corporation
6352 N. Irwindale Avenue
Box 296
Azusa, California (1)

ARO, Inc.
Tullahoma, Tennessee
Attn: Dr. R. W. Perry,
Mr. R. Smelt (1)

AVCO Manufacturing Company
Lycoming Division
Stratford, Connecticut
Attn: Dr. J. C. Keck (1)

Convair
San Diego Division
San Diego, California
Attn: Dr. W. H. Dorrance (1)

Fairchild Engine Division
Fairchild Engine & Aircraft Company
Farmingdale, L.I., New York
Attn: Mrs. C. Minck, Librarian (1)

General Electric Company
Research Laboratory
P. O. Box 1088
Schenectady, New York
Attn: Drs. Nagamatsu, White,
Alpher (1)

The Glenn L. Martin Company
Baltimore 3, Maryland
Department 520, Mail #3072
Attn: Mr. L. Cooper (1)

Hughes Aircraft Corporation
Research & Development Laboratory
Culver City, California
Attn: Dr. A. E. Puckett (1)

Lockheed Aircraft Missile Systems
Division
Van Nuys, California
Attn: Dr. L. Ridenour (1)

Marquardt Aircraft Corporation
7801 Havenhurst
Van Nuys, California (1)

INDUSTRIAL ORGANIZATIONS (cont)

Midwest Research Institute
Department of Physics
4049 Pennsylvania Avenue
Kansas City, Missouri
Attn: Mr. K. L. Sandefur (1)

North American Aviation, Inc.
Aerophysics Department
12214 Lakewood Blvd.
Downey, California
Attn: Dr. van Driest (1)

Ramo-Wooldridge Corporation
8820 Bellanca Avenue
Los Angeles 45, California
Attn: Dr. M. U. Clauser (1)

Rand Corporation
1700 Main Street
Santa Monica, California
Attn: E. P. Williams,
C. Gazley, Jr. (1)

Sandia Corporation
Sandia Base
Albuquerque, New Mexico
Attn: Drs. C. C. Hudson,
M. L. Merritt,
J. D. Shreve, Jr. (1)

Stanford Research Institute
Poulter Laboratories
Stanford, California
Attn: Drs. Poulter, Duvall, Doll (1)

FOREIGN

Institute of Aerophysics
University of Toronto
Toronto 5, Canada
Attn: Dr. G. N. Patterson,
Director (1)

Division of Mechanical Engineering
National Research Laboratories
Ottawa, Canada
Attn: Dr. J. Lukasiewicz (1)

Mr. J. P. Guiraud
Ingenieur de Recherches a' l'
O.N.E.R.A.
De L'Office National D'Etudes et de
Recherches Aeronautiques
29, Avenue de La Division Leglend
CHATILLON-sous-BAGNEUX (Seine)
France (1)